frontiers | Frontiers in Energy Research

TYPE Original Research
PUBLISHED 21 October 2022
DOI 10.3389/fenrg.2022.1028816

OPEN ACCESS

EDITED BY
Nallapaneni Manoj Kumar,
City University of Hong Kong, Hong Kong SAR, China

REVIEWED BY
PremKumar M,
GMR Institute of Technology, India
Jingbo Wang,
University of Liverpool, United Kingdom

*CORRESPONDENCE
Ahmed Fathy,
afali@ju.edu.sa

SPECIALTY SECTION
This article was submitted to Solar Energy, a section of the journal
Frontiers in Energy Research

RECEIVED 26 August 2022
ACCEPTED 04 October 2022
PUBLISHED 21 October 2022

CITATION
Ali HH, Fathy A, Al-Dhaifallah M, Abdelaziz AY and Ebeed M (2022), An efficient capuchin search algorithm for extracting the parameters of different PV cells/modules.
Front. Energy Res. 10:1028816.
doi: 10.3389/fenrg.2022.1028816

An efficient capuchin search algorithm for extracting the parameters of different PV cells/modules

Hossam Hassan Ali[1], Ahmed Fathy[2,3]*, Mujahed Al-Dhaifallah[4,5], Almoataz Y. Abdelaziz[6] and Mohamed Ebeed[7]

[1]Electrical Department, Faculty of Technology and Education, Sohag University, Sohag, Egypt, [2]Electrical Engineering Department, Faculty of Engineering, Jouf University, Sakaka, Saudi Arabia., [3]Electrical Power & Machine Department, Faculty of Engineering, Zagazig University, Zagazig, Egypt, [4]Control and Instrumentation Engineering Department, King Fahd University of Petroleum and Minerals, Dhahran, Saudi Arabia, [5]Interdisciplinary Research Center (IRC) for Renewable Energy and Power Systems, King Fahd University of Petroleum and Minerals, Dhahran, Saudi Arabia, [6]Faculty of Engineering and Technology, Future University in Egypt, Cairo, Egypt., [7]Department of Electrical Engineering, Faculty of Engineering, Sohag University, Sohag, Egypt

Constructing an equivalent circuit for the photovoltaic (PV) generating unit converging the real operation is a difficult process because of unavailability of some parameters. Many approaches have been conducted in this field; however, they have some problems in computational time and are stuck in local optima. Therefore, this study proposes a simple, robust, and efficient methodology-incorporated capuchin search algorithm (CapSA) to construct the equivalent circuit of the PV generating unit *via* identifying its parameters. The CapSA is selected as it is simple and requires less computational time in addition to exploration/exploitation balance that avoids local optima. The process is formulated as an optimization problem, which aims at minimizing the root mean square error (RMSE) between measured and simulated currents. A single-diode model (SDM), double-diode model (DDM), and three-diode model (TDM) of different PV cells and panels operating at either constant or variable weather conditions are constructed. A comparison to different programmed metaheuristic approaches is conducted. The best RMSE values obtained by the proposed CapSA are 2.27804E-04, 1.3808E-04, and 1.5182E-04 for SDM, DDM, and TDM of PVW 752 cell, respectively. For the KC200GT panel, the proposed approach achieved the best fitness values of 3.4440E-04, 1.5617E-03, and 6.6008E-03 at 25°C, 50°C, and 75°C, respectively. The obtained results confirmed the superiority and competence of the proposed CapSA in constructing a reliable equivalent circuit for the PV cell/panel.

KEYWORDS

capuchin search algorithm, PV equivalent circuit, optimization, parameter estimation, renewable energy

1 Introduction

Recently, reliance on renewable energy sources (RESs) has gained great attention to preserve the environment from pollution and reduce global warming. Photovoltaic (PV) cells represent the most widespread renewable energy sources in the world. Although the initial cost of their establishment is high, they have very low operating costs as they do not have any mechanical parts. The PV cells are used to convert the solar radiation into direct electrical energy. The PV generating units are widely used in different applications, such as standalone, microgrids, and large grids with other generating units (Ibrahim et al., 2020; Jiao et al., 2020; Ginidi et al., 2021; Sattar et al., 2021). The PV panels consist of many cells that are connected to each other in series and parallel to obtain the current and voltage required, and the performance of the solar cell is affected by the change in temperature and the intensity of solar radiation (Long et al., 2021). The PV solar cell modeling has been carried out through the following steps: selecting the type of equivalent circuit, describing the equations of the selected model, and identifying the optimal parameters of the equivalent circuit. To improve the performance of solar cells, it is necessary to obtain the optimal values of the parameters *via* analyzing the current–voltage curve and the type of model used (Said et al., 2021). Different models have been constructed for the PV cell, such as a single-diode model (SDM), which requires the definition of five parameters, double-diode model (DDM) with seven parameters to be estimated, and three-diode model (TDM) that involves nine parameters (Wang and Huang, 2018; Premkumar et al., 2021b). The diode reverse saturation current has been considered as the initial parameter employed in calculating the SDM (Şentürk, 2018). Many numerical methods have been conducted to estimate the parameters of the solar cell equivalent circuit, and the Lambert W function has been presented to compute the parameters of the SDM (Ćalasan et al., 2020). Linear least square was used to identify the PV panel parameters using two steps (Reddy and Yammani, 2021). The Newton–Raphson's maximum likelihood approach has been used to construct the PV cell SDM equivalent circuit *via* extracting the unknown parameters (Ayang et al., 2019). An iterative approach with two steps has been employed to calculate the SDM parameters using the panel datasheet; the first step was determining the diode ideality factor, and the second step was estimating the model shunt resistance (Stornelli et al., 2019). Many optimization approaches have been applied to extract the parameters of the PV cells/modules, such as drone squadron optimization incorporated with the Newton–Raphson approach, which has been applied with six states of polycrystalline and monocrystalline SDM and DDM; moreover, one state under different operation condition has been investigated (Gnetchejo et al., 2021). A hybrid approach of whale optimization (WO) and particle swarm optimization (PSO) has been presented to solve the problem of evaluating the unknown parameters for both SDM and DDM for the PV panel (Sharma et al., 2021). A stochastic fractal search optimization (SFSO) has been applied to determine the SDM and DDM circuits' parameters with experimental data of the ESP-160 PPW PV panel (Rezk et al., 2021). An improved grasshopper optimization algorithm (GOA) with lévy flight has been used to obtain the parameters of SDM and DDM for RTC and sharp ND-R250A5 PV panels under different temperatures and solar irradiances (Mokeddem, 2021). Different types of PV modules with SDM, DDM, and TDM circuits have been

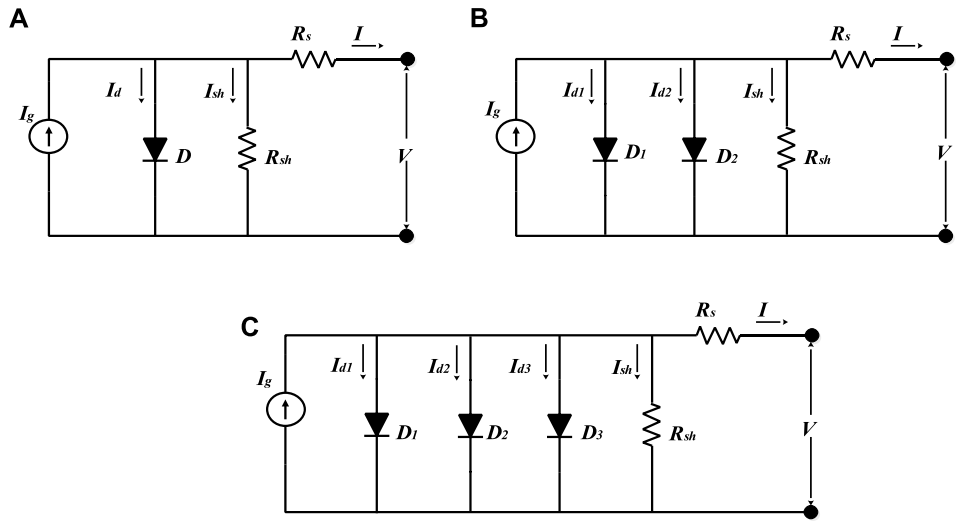

FIGURE 1
Equivalent circuits of the PV cell. **(A)** SDM, **(B)** DDM, and **(C)** TSM.

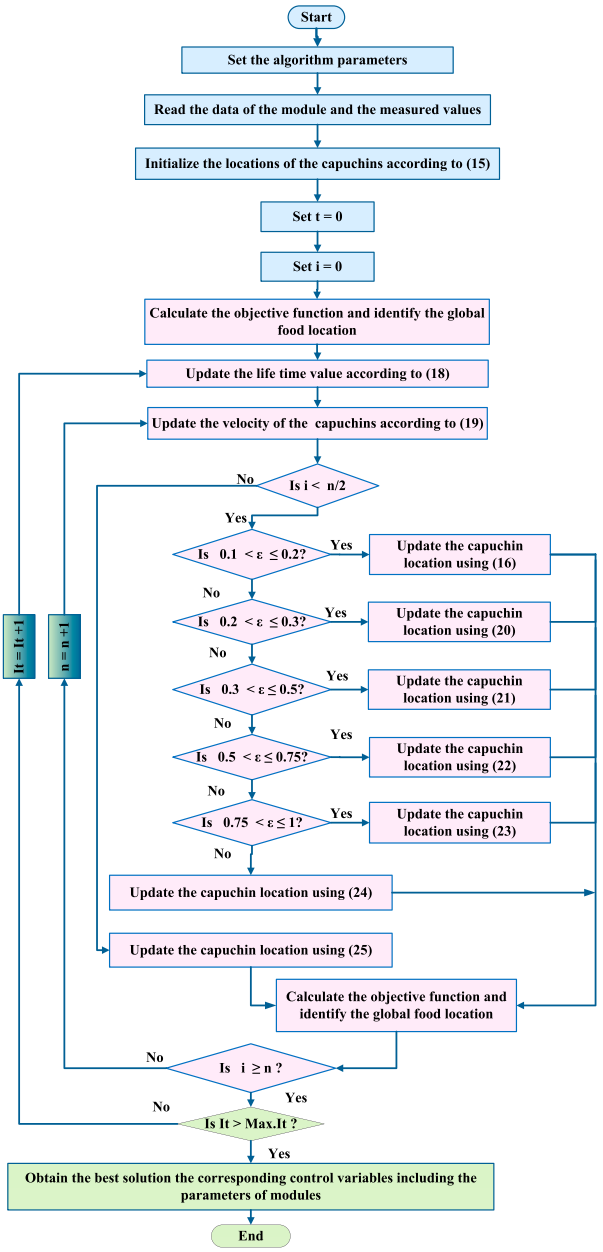

FIGURE 2
Flow chart of the proposed CapSA.

analyzed at various operating conditions with the aid of an artificial ecosystem optimizer (AEO) (Yousri et al., 2020). A gradient-based optimizer (GBO) (Ismaeel et al., 2021), enhanced GOA by metaphor free with ranking mechanisms (Ahmadianfar et al., 2021), improved GOA with opposition (Premkumar et al., 2021a), and enhanced GBO algorithm by chaotic drifts (Premkumar et al., 2021b) have been applied to identify the parameters of different PV cells/modules under different operating conditions. A turbulent flow of water optimizer (TFWO) has been used to estimate the PV equivalent circuit parameters (Abdelminaam et al., 2021; Said et al., 2021). Moreover, bald eagle search (BES) (Nicaire et al., 2021), improved BES (Ramadan et al., 2021a), hybrid grey wolf and cuckoo search (HGWOCS) (Long et al., 2020a), artificial bee colony (ABC)-based teaching learning (Chen et al., 2018), gorilla troop optimizer (Ginidi et al., 2021), and the whale optimization algorithm-based refraction learning (Long et al., 2020b) have been employed to construct the SDM-based circuit of the PV panel. Furthermore, the JAYA algorithm was enhanced *via* guided JAYA, chaotic JAYA, and elite opposition JAYA and employed for estimating the parameters of the PV panels (Wang and Huang, 2018; Yu et al., 2019; Premkumar et al., 2021c). The TDM of the PV system has been presented with the Newton–Raphson approach and the LSHADE algorithm under different operation conditions (Bertalero et al., 2021). The problem of estimating optimal parameters of the PV unit equivalent circuit was presented and solved *via* generalized normal distribution optimization (GNDO) (Zhang et al., 2020), modified jellyfish search optimizer (MJSO) (Abdel-Basset et al., 2021), slime mould algorithm (SMA) (Mostafa et al., 2020), forensic-based investigation algorithm (FBIA) (Shaheen et al., 2021), and chaos game optimization algorithm (CGOA) (Ramadan et al., 2021b). A comprehensive study comprising 28 approaches employed in extracting the PV parameters has been presented in Yang et al. (2020), and a DDM-based circuit of the PV panel has been constructed with the aid of adaptive compass search (ACS) (Zeng et al., 2021). The equivalent circuit of different PV panels has been modeled using an improved equilibrium optimizer based on predictive output data by the back propagation neural network (Wang et al., 2021). An improved GBO with chaotic maps and self-adaptive weighting has been used to estimate the optimal parameters of the PV generating unit (Jiang et al., 2022). A hybrid sine–cosine algorithm (SCA) with differential GBO was introduced to estimate the PV parameters, whereas the differential evolution (DE) and SCA are used to avoid being stuck in local optima and get the global solution (Yu et al., 2022). An approach of hunger games search optimizer (HGSO) with mutation of Cauchy- and Gaussian-based improved Newton–Raphson method has been applied to build and analyze the TDM circuit of the PV panel (Premkumar et al., 2022).

Most reported approaches suffer from some limitations, such as falling in local optima, requiring large consumed time, complicated construction and execution, and requiring many controlling parameters defined by the user, and may cause divergence from the global solution.

These gaps are covered in this work by proposing a novel methodology-incorporated capuchin search algorithm (CapSA) to identify the unknown parameters of the PV cells/panels equivalent circuits. The CapSA is characterized by simplicity, acceptable

TABLE 1 Lower and upper bounds of different PV cells/panels.

Parameters	R.T.C France		PVW 752		PWP-201		STM6-40/36		STP6-120/36		KC200GT	
	Lb	Ub	Lb	Ub	Lb	Ub	Lb	Ub	Lb	Ub	Lb	Ub
a1, a2, and a3	1	2	1	2	1	50	1	60	1	50	1	2
Rs	0	0.5	0	0.8	0	2	0	0.36	0	0.36	0	2
Rsh	0	100	0	1000	0	2000	0	1000	0	1500	0	500
Idr1, Idr2, and Idr3	0	1E-6	0	1E-6	0	50E-6	0	50E-6	0	50E-6	0	10E-6
Ig	0	1	0	0.5	0	2	0	2	0	8	0	16.4

TABLE 2 SDM optimal parameters of R.T.C France and PVW752 PV cells.

Type	Alg	a_1	R_s	R_{sh}	I_{dr1}	I_g	RMSE	Time(s)
R.T.C France	CapSA	1.48119	0.03638	53.71853	3.230E-07	0.76078	9.86022E-04	546.60
	MVO	1.99487	0.01452	99.80331	1.414E-05	0.76728	9.44402E-03	826.90
	EO	1.71048	0.00000	1.14891	0.000E+00	0.83682	2.22861E-01	1440.4
	LAPO	1.48119	0.03638	53.71852	3.230E-07	0.76078	9.86022E-04	1512.0
	HAS	1.59440	0.03191	99.99443	9.180E-07	0.76083	2.28076E-03	3092.0
	SCA	1.60901	0.00000	1.14943	0.000E+00	0.83667	2.22861E-01	724.70
	TSA	1.46889	0.03730	52.91597	2.863E-07	0.76134	1.31104E-03	686.70
PVW752	CapSA	1.61567	0.66051	608.0099	3.779E-12	0.10007	2.27804E-04	591.10
	MVO	1.99491	0.29549	95.5670	3.428E-10	0.10213	3.53887E-03	1045.6
	EO	2.00000	0.00000	14.5886	0.000E+00	0.11376	2.53996E-02	1561.4
	LAPO	1.61568	0.66052	608.8061	3.779E-12	0.10006	2.27820E-04	1569.3
	HAS	1.73075	0.62114	806.4701	1.865E-11	0.09997	3.12100E-04	2731.1
	SCA	1.30046	0.00000	14.5879	0.000E+00	0.11375	2.53996E-02	838.70
	TSA	1.63336	0.64974	415.7086	4.902E-12	0.10052	3.54625E-04	830.40

computation time, and less controlling parameters, and these merits encourage the authors to use the approach to guarantee reliable equivalent circuit that matches to the actual operation. Moreover, a balance between the exploration and exploitation phases of the algorithm enables it to perform well and obtain efficient results.

The main contributions of this work can be summarized as follows:

1) A new approach of CapSA is proposed to extract the optimal parameters of the PV cells/panels equivalent circuits.
2) The proposed CapSA is applied to construct various SDM, DDM, and TDM circuits of the PV system.
3) Comparison to MVO, LAPO, SCA, TSA, EO, and HSA is conducted.
4) The robustness of the proposed CapSA is confirmed through the fetched results.

The article is outlined as follows: Section 2 describes the mathematical model of the PV module, Section 3 introduces the problem formulation, Section 4 clarifies the main principles of CapSA, Section 5 presents the simulation results, and conclusions are given in Section 6.

2 Mathematic model of the photovoltaic module

Three models of PV generating unit are examined: single, double, and three diodes (SDM, DDM, and TDM). These models are widely used to simulate the performance of the solar cell and the panel, and the PV models can be described as follows.

2.1 Single-diode model

In this model, the PV cell is simulated by a current source in parallel with a diode and a shunt resistance, and all are connected

TABLE 3 DDM optimal parameters of R.T.C France and PVW752 PV cells.

Type	Alg	a_1	a_2	R_s	R_{sh}	I_{dr1}	I_{dr2}	I_g	RMSE	Time(s)
R.T.C France	CapSA	2.0000	1.4510	0.0367	55.4854	7.493E-07	2.260E-07	0.76078	9.8248E-04	605.30
	MVO	2.0000	1.4784	0.0359	61.8300	6.237E-07	3.014E-07	0.76102	1.0951E-03	1046.1
	EO	1.9993	1.4780	0.0364	54.0446	9.101E-08	3.109E-07	0.76077	9.8529E-04	1550.8
	LAPO	1.4511	1.9999	0.0367	55.3546	2.263E-07	7.490E-07	0.76079	9.8276E-04	1488.4
	HAS	1.5232	1.8152	0.0339	84.4493	4.446E-07	4.020E-07	0.76033	1.5898E-03	2733.0
	SCA	1.0251	1.5307	0.0341	77.8213	0.000E+00	5.214E-07	0.76246	2.5492E-03	738.00
	TSA	1.6398	1.5207	0.0347	54.9187	9.253E-11	4.728E-07	0.76168	1.3679E-03	761.80
PVW752	CapSA	2.00000	1.00000	0.74432	1000.00	1.897E-10	7.386E-19	0.09991	1.3808E-04	676.50
	MVO	2.00000	1.15690	0.52099	471.723	3.798E-10	0.000E+00	0.10080	8.4986E-04	1011.1
	EO	2.00000	1.08700	0.00000	14.5886	0.000E+00	0.000E+00	0.11376	2.5400E-02	1903.6
	LAPO	1.99977	1.08526	0.73202	830.747	1.747E-10	1.665E-17	0.09996	1.5014E-04	1855.1
	HAS	1.74489	1.64269	0.64484	549.211	3.058E-12	4.834E-12	0.10022	2.5862E-04	3043.2
	SCA	1.63432	2.00000	0.00000	14.6064	0.000E+00	0.000E+00	0.11371	2.5400E-02	897.80
	TSA	1.74182	1.33334	0.61685	489.247	2.142E-11	0.000E+00	0.10047	4.1928E-04	885.80

TABLE 4 TDM optimal parameters of R.T.C France and PVW752 PV cells.

Type	Alg	a_1	a_2	a_3	R_s	R_{sh}	I_{dr1}	I_{dr2}	I_{dr3}	I_g	RMSE
R.T.C France	CapSA	2.0000	1.4510	2.0000	0.0367	55.4854	5.30E-07	2.26E-07	2.19E-07	0.76078	9.8248E-04
	MVO	1.0437	1.4661	1.9988	0.0365	61.2724	0	2.69E-07	4.63E-07	0.76055	1.0249E-03
	EO	1.9999	1.4521	2.0000	0.0367	55.4253	0	2.29E-07	7.24E-07	0.76078	9.8249E-04
	LAPO	1.9998	1.9993	1.4433	0.0368	56.0084	8.38E-07	8.34E-08	2.06E-07	0.76078	9.8274E-04
	HAS	1.5715	1.9886	1.4977	0.0354	60.7847	3.08E-08	1.51E-07	3.60E-07	0.76063	1.1034E-03
	SCA	1.4915	1.0000	1.5742	0.0339	83.1481	0	0	7.69E-07	0.76040	3.2370E-03
	TSA	1.5836	2.0000	1.3410	0.0375	57.8322	3.17E-07	8.20E-07	3.94E-08	0.76039	1.1321E-03
PVW752	CapSA	1.0617	1.9996	2.0000	0.7318	1000.000	7.17E-18	1.80E-10	4.82E-12	0.0999	1.5182E-04
	MVO	1.1439	2.0000	1.6729	0.5149	394.825	0	3.76E-10	0	0.1007	9.0585E-04
	EO	1.2866	1.6385	1.5413	0.6528	678.934	0	5.28E-12	0	0.1000	2.3209E-04
	LAPO	1.2463	1.1068	2.0000	0.6961	1000.000	1.74E-15	4.03E-23	1.67E-10	0.0999	1.9479E-04
	HAS	1.9998	1.3751	1.9501	0.5421	999.690	5.92E-15	2.20E-16	2.32E-10	0.1001	6.2030E-04
	SCA	1.4576	2.0000	1.9497	0.0000	14.579	0	0	0	0.1138	2.5400E-02
	TSA	2.0000	1.5109	2.0000	0.6979	651.825	5.57E-14	7.13E-13	7.13E-13	0.0997	3.7605E-04

in series with a resistance, as shown in Figure 1 (a); the output current of the cell can be described by the following equations (Low and Soon, 2012; Fathy and Rezk, 2017):

$$I = I_g - I_d - I_{sh}, \tag{1}$$

$$I = I_g - I_d\left(exp\left(\frac{q(V + IR_s)}{akT} - 1\right)\right) - \frac{(V + IR_s)}{R_{sh}} \tag{2}$$

where V, I_g, I_d, R_{sh}, and R_s are the output voltage, light generated current, diode reverse saturation current, shunt resistance, and series resistance, respectively; a is the ideality factor of the diode; q denotes the electron charge (q = 1.60217646 × 10^{-19} C); k is the constant of Boltzmann constant (k = 1.3806503 × 10^{-23} J/K); and T indicates the temperature in Kelvin. The parameters to be identified in this model are a, R_s, R_{sh}, I_d, and I_g.

2.1.1 Double-diode model

The equivalent circuit of the DDM of the PV cell is shown in Figure 1 (b). In this model, a second diode is used to simulate the effects of recombination, whereas the first one represents the current of diffusion. The output current can be calculated as follows (Askarzadeh and Rezazadeh, 2013; Alam et al., 2015):

$$I = I_g - I_{d1} - I_{d2} - I_{sh}, \tag{3}$$

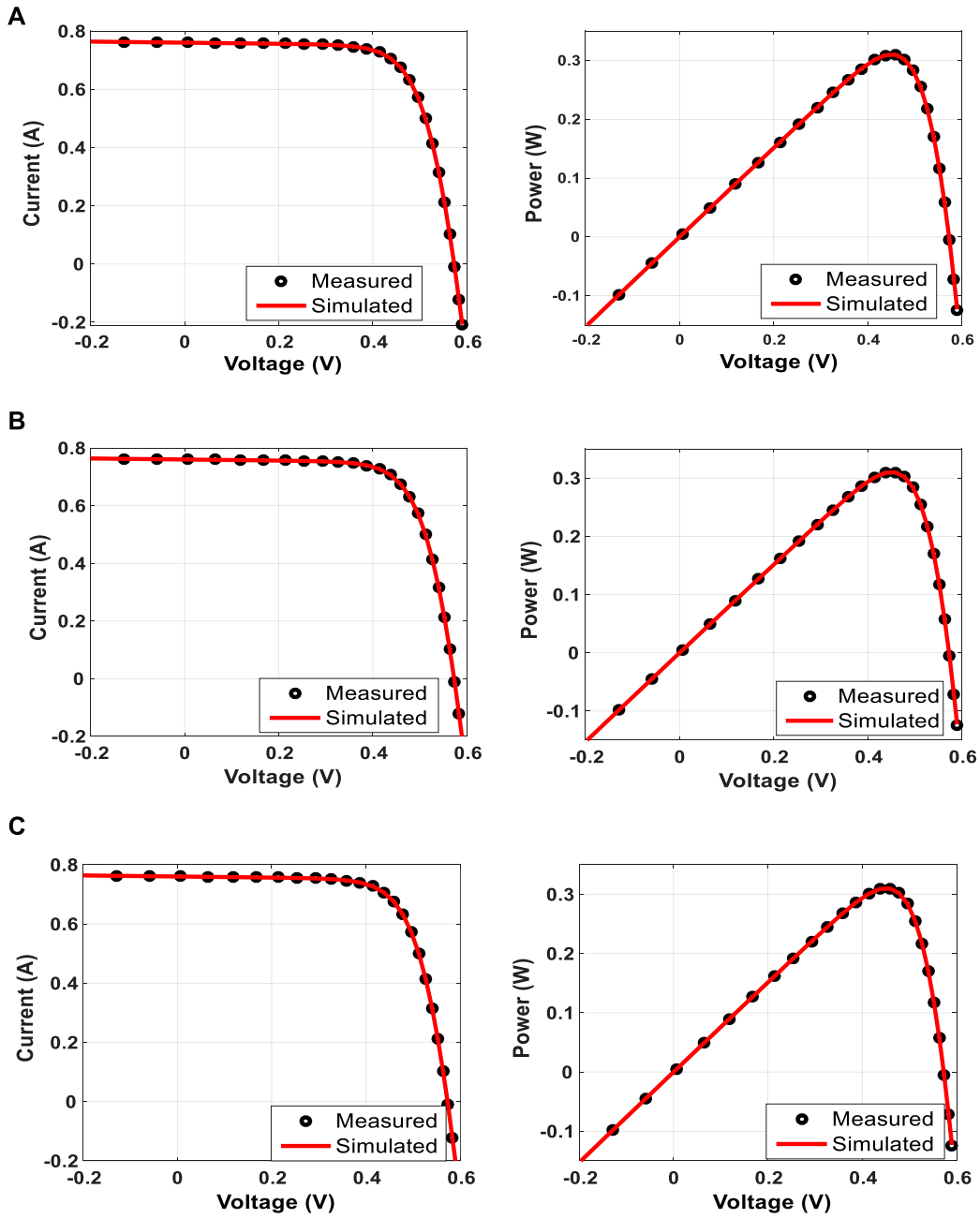

FIGURE 3
Measured and simulated curves obtained *via* CapSA for the R.T.C France PV cell. **(A)** SDM, **(B)** DDM, and **(C)** TDM.

$$I = I_g - I_{d1}\left(exp\left(\frac{q(V+IR_s)}{a_1kT}\right)-1\right) - I_{d2}\left(exp\left(\frac{q(V+IR_s)}{a_2kT}\right)-1\right) - \frac{(V+IR_s)}{R_{sh}} \quad (4)$$

where I_{d1} and I_{d2} are the diodes' reverse saturation currents, and a_1 and a_2 are the ideality factors of the diodes. The DDM has seven parameters to be estimated, which are a_1, a_2, R_s, R_{sh}, I_{d1}, I_{d2}, and I_g.

2.1.2 Three-diode model

The equivalent circuit of the TDM is shown in Figure 1 (c). The third diode is used to simulate the leakage current. The output current in such a model can be described as follows (Yousri et al., 2020):

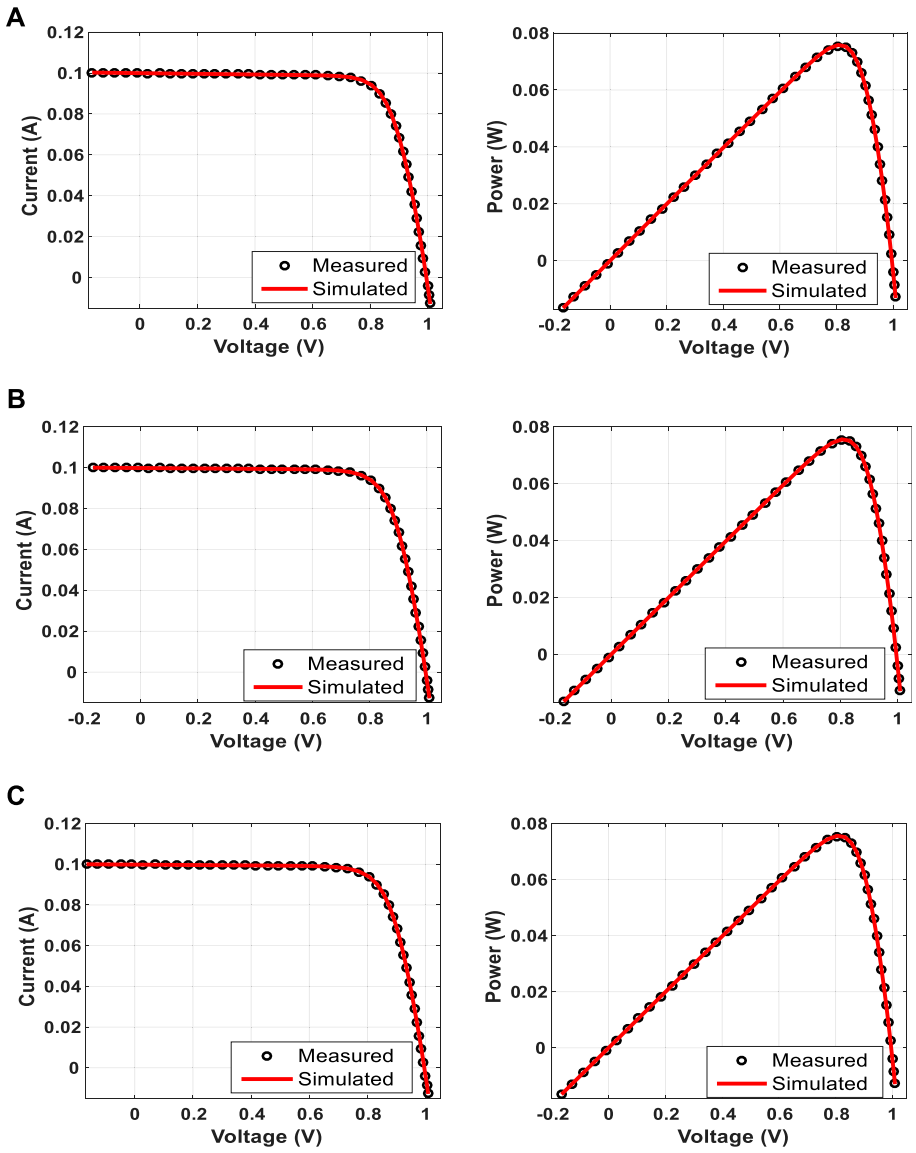

FIGURE 4
Measured and simulated I–V and P–V curves of the PVM752 cell. **(A)** SDM, **(B)** DDM, and **(C)** TDM.

$$I = I_g - I_{d1} - I_{d2} - I_{d3} - I_{sh}, \tag{5}$$

$$I = I_g - I_{d1}\left(exp\left(\frac{q(V+IR_s)}{a_1 kT}\right) - 1\right) - I_{d2}\left(exp\left(\frac{q(V+IR_s)}{a_2 kT}\right) - 1\right) - I_{d3}\left(exp\left(\frac{q(V+IR_s)}{a_3 kT}\right) - 1\right) - \frac{(V+IR_s)}{R_{sh}}, \tag{6}$$

where I_{d3} and a_3 are the third diode reverse saturation current and its ideality factor. It is noticeable that Eq. 6 contains nine parameters to be identified: a_1, a_2, a_3, R_s, R_{sh}, I_{d1}, I_{d2}, I_{d3}, and I_g.

3 Problem formulation

Estimating the parameters of the PV equivalent circuit is formulated as an optimization problem, and the considered fitness function to be minimized is root mean square error (RMSE) between the measured and simulated currents. The undefined parameters represent the design variables in the formulated optimization problem. The main target is constructing a reliable circuit with confident I–V curves that converge to the experimental data (Ram et al., 2017; Yu et al., 2018; El-Fergany, 2021). The fitness function can be written as follows:

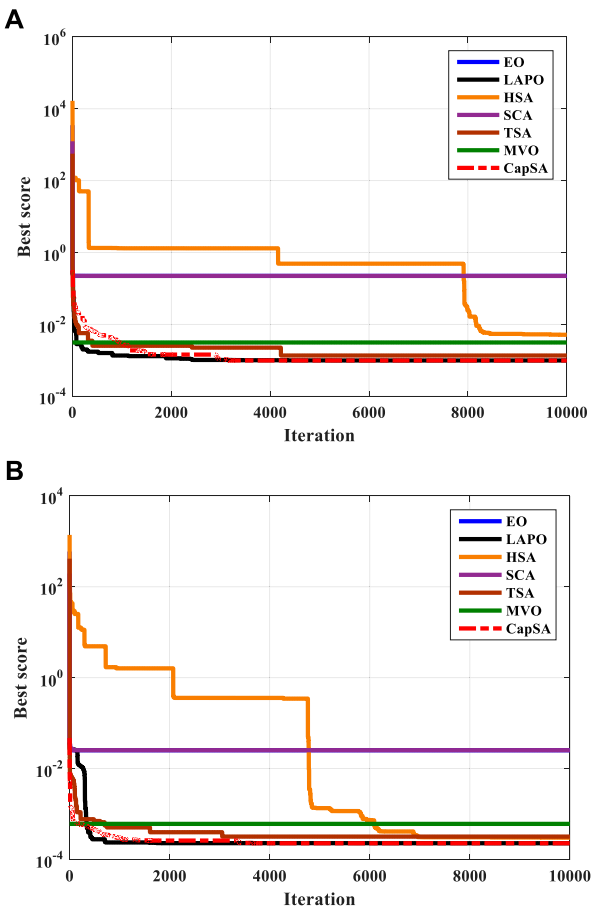

FIGURE 5
Convergence curves of the fitness function obtained *via* different optimizers. **(A)** R.T.C France cell and **(B)** PVW752 cell.

$$RMSE_{PV} = \sqrt{\frac{1}{N}\sum_{i=1}^{N} f_{PV}(V,I,x)^2} = \sqrt{\frac{1}{N}\sum_{i=1}^{N} (I_{meas} - I_{sim})^2}, \tag{7}$$

where f_{PV} denotes the function of PV unit, N denotes the nuebr of measured data, I_{meas} is the measured current, and I_{sim} indicates the simulated current.

3.1 Fitness function of the single-diode model

The fitness function employed to construct the SDM-based circuit of the PV system can be described as follows:

$$f_{SDM}(V,I,x) = I - x_5 + x_4\left(exp\left(\frac{q(V+Ix_2)}{x_1 kT} - 1\right)\right) + \frac{(V+Ix_2)}{x_3} \tag{8}$$

TABLE 5 Statistical parameters of the approaches applied to PVM752 PV cell.

Type	Alg	Min	Max	Mean	Std
SDM	CapSA	2.2780E-04	2.2780E-04	2.2780E-04	8.1938E-18
	MVO	3.5389E-03	2.5399E-02	1.9287E-02	9.1856E-03
	EO	2.5399E-02	2.5399E-02	2.5399E-02	1.4691E-17
	LAPO	2.2782E-04	2.6106E-04	2.2937E-04	6.0143E-06
	HAS	3.1210E-04	3.8402E-01	7.8755E-02	9.5693E-02
	SCA	2.5399E-02	2.5400E-02	2.5399E-02	1.9359E-07
	TSA	3.5463E-04	2.5399E-02	3.3489E-03	7.5611E-03
DDM	CapSA	1.3808E-04	7.9369E-04	2.2342E-04	1.1954E-04
	MVO	8.4986E-04	2.5399E-02	1.2188E-02	9.6925E-03
	EO	2.5399E-02	2.5399E-02	2.5399E-02	1.7644E-17
	LAPO	1.5014E-04	2.7024E-03	3.6194E-04	4.6635E-04
	HAS	2.5862E-04	7.6665E-01	2.3147E-01	1.8403E-01
	SCA	2.5399E-02	2.5400E-02	2.5399E-02	1.6299E-07
	TSA	4.1928E-04	6.6432E-03	8.7682E-04	1.0949E-03
TDM	CapSA	1.5182E-04	7.3492E-04	2.2634E-04	1.2863E-04
	MVO	9.0585E-04	2.5399E-02	1.2508E-02	8.6417E-03
	EO	2.3209E-04	2.5399E-02	2.4561E-02	4.5949E-03
	LAPO	1.9479E-04	2.5399E-02	1.1962E-02	1.2161E-02
	HAS	6.2030E-04	1.8121E+00	6.5578E-01	4.4943E-01
	SCA	2.5399E-02	2.5400E-02	2.5399E-02	1.2154E-07
	TSA	3.7605E-04	1.2107E-02	1.4843E-03	2.5089E-03

where x is a vector of design variables (a, R_s, R_{sh}, I_d, and I_g).

3.2 Fitness function of the double-diode model

In DDM, the considered fitness function is written as follows:

$$f_{DDM}(V,I,x) = I - x_7 + x_5\left(exp\left(\frac{q(V+Ix_3)}{x_1 kT}\right) - 1\right) + x_6\left(exp\left(\frac{q(V+Ix_3)}{x_2 kT}\right) - 1\right) + \frac{(V+Ix_3)}{x_4}, \tag{9}$$

where x includes seven parameters: a_1, a_2, R_s, R_{sh}, I_{d1}, I_{d2}, and I_g.

3.3 Fitness function of the three-diode model

In such a model, nine parameters (a_1, a_2, a_3, R_s, R_{sh}, I_{d1}, I_{d2}, I_{d3}, and I_g) represent the design variables, and they are introduced as x vector; the fitness function considered in such model can be given as follows:

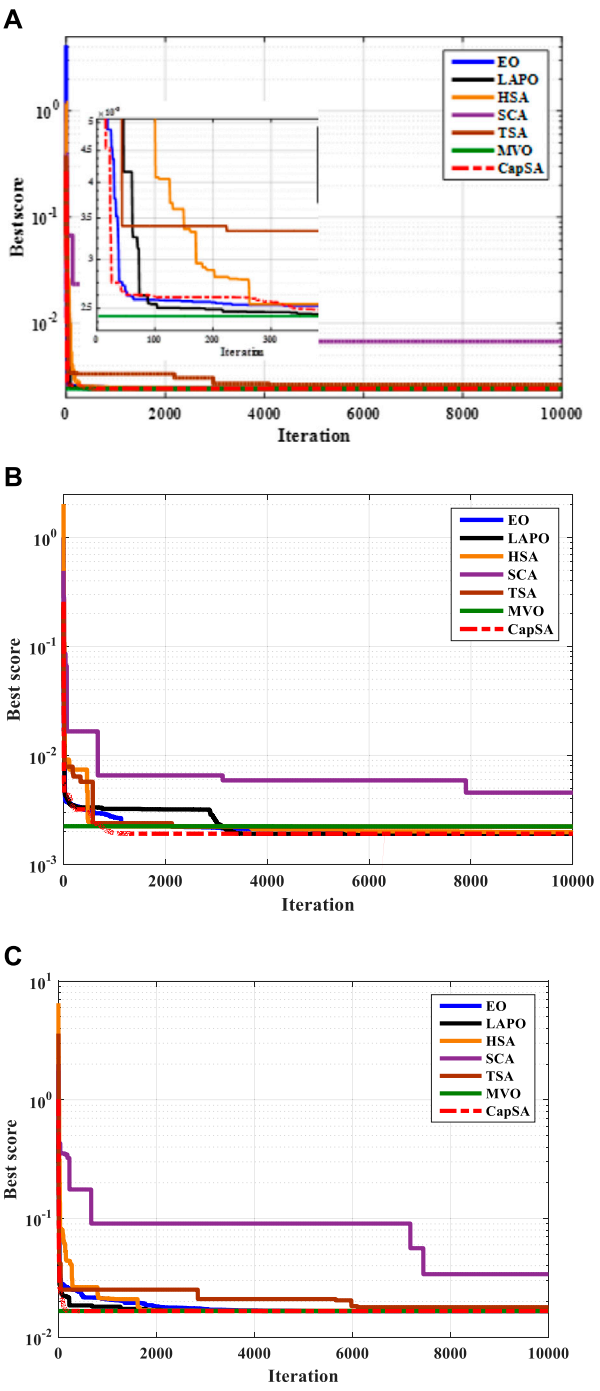

FIGURE 6
Fitness value versus iteration number for **(A)** PWP-201, **(B)** STM6-40/36, and **(C)** STP6-120/36 panels.

$$f_{TDM}(V,I,x) = I - x_9 + x_6\left(exp\left(\frac{q(V+Ix_4)}{x_1kT}\right) - 1\right) + x_7\left(exp\left(\frac{q(V+Ix_4)}{x_2kT}\right) - 1\right) + x_8\left(exp\left(\frac{q(V+Ix_4)}{x_3kT}\right) - 1\right) + \frac{(V+Ix_4)}{x_5}. \quad (10)$$

4 Capuchin search algorithm

The capuchin search algorithm (CapSA) is a novel optimizer that mimics the foraging behavior of the capuchins for searching the food resources over the branches of trees and riverbanks (Braik et al., 2021). During the foraging process, capuchins leap, climb, and swing to search for food. They are social animals that move in the forest as family, where they are live in groups with adult female, male, and small apes. Capuchins' movements in the forest to find the most abundant food location simulate the global search optimization algorithms. In the foraging, they interact with their leader and with each other by calling, barking, and postures. CapSA can be modeled based on three mechanisms of the motion, as follows.

4.1 Leaping motion

Capuchins move long distances over trees to find and discover food resources; this is similar to the global search mechanism. Here, movement of the capuchins between tress looks like the projectile motion, which can be expressed by the third law of motion, as follows:

$$x_m = x_0 + v_0 t + \frac{1}{2}at^2, \quad (11)$$

where x_m, x_0, v_0, and t are the capuchin new location, initial location, initial speed, and time, respectively. This equation can be modified as follows:

$$x_m = x_0 + v_0^2 \sin(2\theta_0)/g \quad (12)$$

where g denotes the gravitational acceleration and θ_0 denotes leaping angle.

4.1.1 Swinging motion

Capuchins wobble on branches of the trees in the foraging process; this action simulates the pendulum motion. This motion mimics the local search phase, and it can be described as follows:

TABLE 6 SDM optimal parameters of PWP-201, STM6-40/36, and STP6-120/36 panels.

Type	Alg	a_1	R_s	R_{sh}	I_{dr1}	I_g	RMSE	Time(s)
PWP-201	CapSA	48.64290	1.20127	981.9822	3.482E-06	1.03051	2.42507E-03	517.50
	MVO	48.54071	1.20430	946.9971	3.390E-06	1.03076	2.42669E-03	845.20
	EO	48.69365	1.19999	1004.0137	3.529E-06	1.03037	2.42544E-03	1460.3
	LAPO	48.64290	1.20127	981.9825	3.482E-06	1.03051	2.42507E-03	1595.9
	HAS	48.91044	1.19273	934.4454	3.730E-06	1.03150	2.46479E-03	2702.7
	SCA	50.00000	1.18974	1089.2080	4.934E-06	1.03615	4.78058E-03	745.70
	TSA	48.91044	1.19273	934.4454	3.730E-06	1.03150	2.64948E-03	763.20
STM6-40/36	CapSA	53.12697	0.21794	543.7935	1.147E-06	1.66440	1.90610E-03	542.80
	MVO	52.73569	0.22860	518.9537	1.032E-06	1.66498	1.92725E-03	868.60
	EO	53.04984	0.21991	537.6140	1.123E-06	1.66455	1.90725E-03	1493.1
	LAPO	53.12698	0.21794	543.7936	1.147E-06	1.66440	1.90610E-03	1464.3
	HAS	53.53326	0.20951	607.2201	1.280E-06	1.66265	2.02727E-03	2691.2
	SCA	60.00000	0.00000	1000.0000	5.859E-06	1.65983	4.58893E-03	731.40
	TSA	51.61589	0.25873	491.9739	7.553E-07	1.66470	2.20758E-03	712.00
STP6-120/36	CapSA	45.36378	0.16541	799.9165	2.335E-06	7.47253	1.66006E-02	445.40
	MVO	45.33650	0.16549	743.8446	2.314E-06	7.47340	1.66024E-02	698.30
	EO	45.40730	0.16519	880.7132	2.369E-06	7.47144	1.66024E-02	1168.0
	LAPO	45.36378	0.16541	799.9167	2.335E-06	7.47253	1.66006E-02	1190.0
	HAS	45.80751	0.16286	927.7289	2.701E-06	7.47380	1.67470E-02	2160.4
	SCA	47.08395	0.15794	384.7876	3.999E-06	7.48488	3.04560E-02	562.10
	TSA	45.89616	0.16120	484.6761	2.785E-06	7.48577	1.76709E-02	568.80

$$\boldsymbol{x} = \boldsymbol{L}\,\mathbf{sin}\ \boldsymbol{\theta}, \tag{13}$$

where L is the length of tail and θ denotes the swing angle of capuchin.

4.1.2 Climbing motion

The capuchins climb to the trees for searching the food resources, and this motion mimics the local searching process in the optimization approach. The climbing motion is described as follows:

$$\boldsymbol{x_m} = \boldsymbol{x_0} + \boldsymbol{v_0 t} + \mathbf{0.5}(\boldsymbol{v} - \boldsymbol{v_0})\boldsymbol{t^2}. \tag{14}$$

The initial locations of the capuchins can be calculated as follows:

$$\boldsymbol{X^i} = \boldsymbol{X^{Lb}} + \left(\boldsymbol{X^{Ub}} - \boldsymbol{X^{Lb}}\right) \times \boldsymbol{rand}, \tag{15}$$

where X^{Lb} is the lower limit of the control variable while X^{Ub} is its upper limit and *rand* is a random number within [0, 1]. The group of the capuchin has two types of the populations: the leader or the alpha and the followers. Both of them search food resource, denoted as F. Other capuchins may also join the leader in the foraging behavior and pursue similar locomotion behavior. The leader jumps between the branches to find the source food, and this can be expressed as follows:

$$\boldsymbol{X^i} = \boldsymbol{F} + \frac{\boldsymbol{P_{bf}}\left(\boldsymbol{v^i}\right)^2 \boldsymbol{sin}\left(\mathbf{2}\boldsymbol{\theta_j}\right)}{\boldsymbol{g}}, \quad \boldsymbol{i} < \frac{\boldsymbol{n}}{\mathbf{2}}; \mathbf{0.1} < \boldsymbol{\varepsilon} \le \mathbf{0.2}, \tag{16}$$

where P_{bf} is the probability of the balance provided by the capuchins tail, ε is a random number, and θ_j deotes the capuchin's jumbing angle, which is given as follows:

$$\theta_j = \frac{\mathbf{3}}{\mathbf{2}}\boldsymbol{r}, \tag{17}$$

where r is a random value within [0, 1]. To achieve balance between exploration and exploitation of the CapSA, an operator (τ) represents the life time of the CapSA, and it can cause balance between the global and local searching phases; this operator can be calculated as follows:

$$\boldsymbol{\tau} = \boldsymbol{\beta_0 e}^{-\boldsymbol{\beta_1}\left(\frac{Iter}{max\ \_Iter}\right)^{\boldsymbol{\beta_2}}}, \tag{18}$$

where *Iter* denotes the current iteration while *max _Iter* is the maximum number of iterations; β_0, β_1, and β_2 are random numbers with values of 2, 21, and 2, respectively. The velocity of the capuchin can be calculated as follows:

TABLE 7 DDM optimal parameters of PWP-201, STM6-40/36, and STP6-120/36 panels.

Type	Alg	a_1	a_2	R_s	R_{sh}	I_{dr1}	I_{dr2}	I_g	RMSE	Time (s)
PWP-201	CapSA	48.6743	14.9924	1.2284	1084.581	3.476E-06	1.945E-20	1.0301	2.3306E-03	535.00
	MVO	48.5111	23.7948	1.2044	933.4204	3.364E-06	0.000E+00	1.0308	2.4274E-03	731.90
	EO	5.9281	48.6622	1.2008	988.9690	0.000E+00	3.500E-06	1.0305	2.4251E-03	1551.7
	LAPO	33.7156	48.6429	1.2013	981.9840	8.136E-21	3.482E-06	1.0305	2.4251E-03	1567.5
	HAS	49.4517	48.3887	1.1890	1331.118	3.257E-06	7.870E-07	1.0289	2.4766E-03	2806.5
	SCA	19.0793	50.0000	1.1734	678.2340	0.000E+00	4.840E-06	1.0308	6.5520E-03	668.50
	TSA	50.0000	50.0000	1.1585	1276.919	1.093E-06	3.821E-06	1.0297	2.7169E-03	665.30
STM6-40/36	CapSA	36.5339	60.0000	0.3600	603.186	8.196E-10	3.240E-06	1.66427	1.7309E-03	548.70
	MVO	52.1984	33.6318	0.2429	486.471	8.898E-07	0.000E+00	1.66591	2.0292E-03	763.10
	EO	50.7648	60.0000	0.2310	550.308	4.611E-07	1.296E-06	1.66437	1.8816E-03	1172.7
	LAPO	43.5677	59.0559	0.2718	584.705	2.376E-08	2.556E-06	1.66395	1.8265E-03	1334.1
	HAS	55.0330	54.2329	0.1731	621.230	1.054E-06	6.735E-07	1.66326	2.1265E-03	2612.5
	SCA	30.5345	60.0000	0.0000	869.296	0.000E+00	5.853E-06	1.66218	4.5854E-03	670.40
	TSA	54.5721	53.6560	0.2012	535.691	4.414E-11	1.319E-06	1.66552	2.0329E-03	640.00
STP6-120/36	CapSA	13.9294	45.4583	0.17061	1500.000	1.108E-22	2.357E-06	7.46837	1.6421E-02	536.40
	MVO	1.0018	45.3100	0.16565	706.131	0.000E+00	2.293E-06	7.47406	1.6604E-02	747.20
	EO	45.3676	50.0000	0.16539	807.981	2.338E-06	0.000E+00	7.47241	1.6601E-02	1232.4
	LAPO	45.3638	47.6348	0.16541	799.910	2.335E-06	2.224E-13	7.47253	1.6601E-02	1384.0
	HAS	44.8293	45.5172	0.16712	581.404	1.375E-06	7.255E-07	7.47586	1.6671E-02	2469.1
	SCA	44.5922	49.8144	0.14131	858.482	0.000E+00	8.985E-06	7.50427	3.3653E-02	676.20
	TSA	45.0246	47.2204	0.16746	438.324	2.019E-06	1.315E-07	7.49236	1.7966E-02	614.70

$$\boldsymbol{v^i = \rho X^i + \tau a_1 \left(X^i_{best} - X^i\right) r_1 + \tau a_2 \left(F - X^i\right) r_2}, \quad (19)$$

where X^i_{best} represents the best location of the ith capuchin, a_1 and a_2 are two positive values that control the effects of F and X^i_{best} on the velocity, r_1 and r_2 are random numbers in [0, 1], and ρ is an inertia coefficient equal to 0.7. The alpha capuchin can jump on wide areas to find food resources when the food on trees decreases. The leader and the other capuchins' motions can be represented as follows:

$$\boldsymbol{X^i = F + \frac{P_{ef} P_{bf} \left(v^i\right)^2 sin\ (2\theta)}{g}}, \quad \boldsymbol{i < n/2\ ; 0.2 < \varepsilon \le 0.3} \quad (20)$$

where P_{ef} is the probability movement of the capuchins on the ground. The motion of the alpha leader on the ground can be expressed as follows:

$$\boldsymbol{X^i = X^i + v^i}, \ \boldsymbol{i < n/2\ ; 0.3 < \varepsilon \le 0.5} \quad (21)$$

The swinging of the capuchins and alpha leader on the trees branches searching the food in the local region can be expressed as follows:

$$\boldsymbol{X^i = F + \tau P_{bf}}, \ \boldsymbol{i < n/2\ ; 0.5 < \varepsilon \le 0.75} \quad (22)$$

Some capuchins and the alpha leader climb the trees and fall several times to find the food as local search, and this can be expressed as follows:

$$\boldsymbol{X^i_j = F_j + \tau P_{bf}\left(v^i_j - v^i_{j-1}\right)}, \ \boldsymbol{i < n/2\ ; 0.75 < \varepsilon \le 1.0} \quad (23)$$

Capuchins also move randomly to explore new areas, which is known as the random relocation of the capuchins, and this can be mathematically described as follows:

$$\boldsymbol{X^i = \tau \times \left[X^{Lb} + \varepsilon \times \left(X^{Ub} - X^{Lb}\right)\right]}, \quad \boldsymbol{i < n/2\ ;\ \varepsilon \le P_r}, \quad (24)$$

where P_r is a constant equal to 0.1. The behavior of the followers update their locations with respect to their leader according to the following equation.

$$\boldsymbol{X^i_j = \frac{1}{2}\left(XL^i_j + X^{i-1}_j\right)}, \ \boldsymbol{\frac{n}{2} \le i \le n}, \quad (25)$$

where XL^i_j and X^{i-1}_j are the leader location and the previous location of follower, respectively. The application of the capuchin search algorithm to estimate the optimal parameters of the PV panel equivalent circuit is depicted in Figure 2.

TABLE 8 TDM optimal parameters of PWP-201, STM6-40/36, and STP6-120/36 panels.

Type	Alg	a_1	a_2	a_3	R_s	R_{sh}	I_{dr1}	I_{dr2}	I_{dr3}	I_g	RMSE (E)
PWP-201	CapSA	14.712	49.293	48.693	1.2362	1140.575	1.12E-20	2.38E-08	3.46E-06	1.0299	2.3240–3
	MVO	47.963	1.044	48.864	1.2165	1021.078	2.17E-06	0	9.39E-07	1.0298	2.4871–3
	EO	50.000	48.632	1.015	1.2016	978.899	0	3.47E-06	0	1.0305	2.4251–3
	LAPO	48.417	48.423	49.943	1.2012	984.447	1.87E-06	9.15E-07	7.36E-07	1.0305	2.4268–3
	HAS	49.980	18.061	48.407	1.2078	923.823	1.11E-11	1.83E-19	3.27E-06	1.0308	2.4307–3
	SCA	29.045	50.000	4.668	1.1319	1145.159	0	4.84E-06	0	1.0210	7.2495–3
	TSA	50.000	50.000	46.426	1.2040	860.209	1.22E-06	1.38E-06	8.92E-07	1.0309	2.5689–3
STM6-40/36	CapSA	60.000	60.000	36.534	0.3600	603.186	3.16E-06	8.02E-08	8.20E-10	1.66427	1.7309–3
	MVO	29.052	2.400	58.674	0.0185	546.868	0	0	4.39E-06	1.66686	2.3882–3
	EO	50.822	59.999	60.000	0.2213	567.083	4.50E-07	0	1.49E-06	1.66412	1.8908–3
	LAPO	58.280	59.462	46.794	0.2569	558.817	3.41E-08	2.17E-06	9.70E-08	1.66430	1.8525–3
	HAS	56.069	56.670	45.690	0.1576	662.019	8.88E-07	1.47E-06	1.21E-08	1.66306	2.3879–3
	SCA	37.014	60.000	10.650	0.0000	1000.000	0	5.88E-06	0	1.65983	4.6561–3
	TSA	60.000	52.686	60.000	0.1683	694.367	5.66E-07	6.96E-07	1.29E-06	1.66127	2.4674–3
STP6-120/36	CapSA	45.2233	50.0000	13.8614	0.1751	1084.273	2.15E-06	8.10E-18	1.38E-22	7.47091	1.6269–2
	MVO	45.5469	11.3142	1.0087	0.1647	1331.971	2.48E-06	0	0	7.46847	1.6645–2
	EO	45.4482	45.3392	49.9963	0.1655	779.379	1.37E-07	2.18E-06	0	7.47279	1.6601–2
	LAPO	50.0000	45.6912	45.3897	0.1653	885.115	3.51E-11	0	2.36E-06	7.47159	1.6605–2
	HAS	43.7030	45.9861	49.7463	0.1683	962.726	8.54E-07	6.88E-07	9.86E-07	7.46713	1.6863–2
	SCA	49.4655	34.3442	43.6289	0.1455	1075.710	8.08E-06	0	0	7.51257	3.1240–2
	TSA	44.7453	50.0000	43.7672	0.1674	1500.000	4.05E-07	1.91E-06	7.91E-07	7.47311	1.7618–2

5 Simulation and results

In this work, the CapSA approach is used to determine the parameters of different PV models. The parameters are identified for SDM, DDM, and TDM models of R.T.C France, PVM752, PWP-201, STM6-40/36, and STP6-120/36 operated at standard test conditions (STCs). On the other hand, the DDM-based circuit of the KC200GT PV module is constructed and investigated under different temperatures and solar irradiances. The fetched results *via* the proposed CapSA are compared to MVO, LAPO, SCA, TSA, EO, and HAS. The considered algorithms are executed for 30 independent runs with controlling parameters of 10,000 maximum iteration and a population size of 50 (Pourmousa et al., 2019). The algorithm is executed for 30 independent runs to minimize the effect of random numbers considered in the algorithm. However, the run with the minimum fitness value is selected as the optimal result. The upper and lower bounds (Ub and Lb) of the identified parameters for different PV cells/panels are presented in Table 1. The measured data of I–V for the considered PV cells/panels are shown in Supplementary Table S1, where the number of samples for R.T.C France is 26; PVM752 is 44; whereas the number of patterns for PWP-201, STM6-40/36, and STP6-120/36 are 25, 20, and 24, respectively. Finally, the number of measured patterns for KC200GT is 15 samples.

5.1 Case 1: Photovoltaic cells

The proposed CapSA is employed to extract the unknown parameters of SDM, DDM, and TDM for the R.T.C France PV cell operated at 33°C and 1000W/m^2 and the PVM752 GaAs thin film cell at 25°C and 1000W/m^2. The measured data of I–V and the cell electric characteristics are given in Gao et al. (2018), Rezaee Jordehi (20180, Yu et al. (2018), Yousri et al. (2020), and Lekouaghet et al. (2021). Table 2 illustrates the optimum parameters and the RMSE value of SDM obtained *via* the proposed CapSA in comparison to other algorithms. The CapSA and LAPO approaches achieved the lowest RMSE value of 9.86022E-04 for the R.T.C France PV cell, whereas the minimum RMSE value of 2.27804E-04 for the PVW752 cell is obtained by a CapSA optimizer. The optimal parameters of DDM obtained *via* the proposed CapSA and others are tabulated in Table 3, and the R.T.C France minimum RMSE value of 9.8248E-04 is obtained by the proposed CapSA. Regarding to the DDM of PVW752 cell, the proposed CapSA comes in the

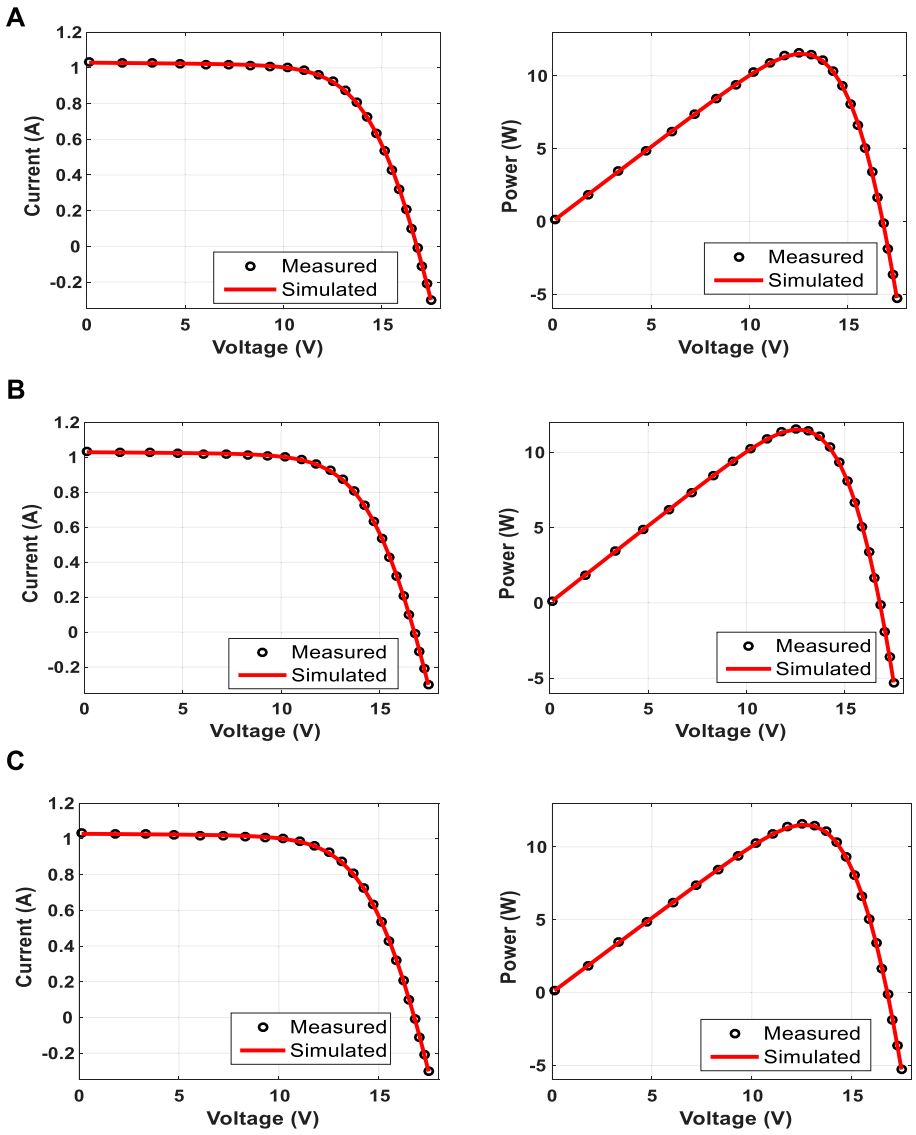

FIGURE 7
Measured and simulated I–V and P–V curves of the PWP-201 PV panel. **(A)** SDM, **(B)** DDM, and **(C)** TDM.

first rank achieving the least RMSE value of 1.3808E-04, whereas the LAPO comes in the second rank with RMSE of 1.5014E-04. Regarding the computational time given in Table 2, the proposed approach achieved the best consumed time of 546.60 s and 591.10 s during establishing the SDM circuit for R.T.C France and PVW752 PV cells, respectively. TSA came second consuming 686.70 s and 830.0 s for both cells, respectively. On the other hand, the HAS had the longest computational time of 686.70 s and 2731.1 s for the two mentioned cells. Moreover, the proposed CapSA outperformed the others in term of computational time during establishing the DDM-based circuit. Moreover, Table 4 presents the parameters of the TDM-based circuit constructed *via* CapSA, MVO, LAPO, SCA, TSA, EO, and HAS. The results presented in Table 4 clarified that the lowest RMSE value of 9.8248E-04 is obtained by the proposed CapSA, whereas the worst RMSE value of 3.2370E-03 is obtained *via* SCA for the R.T.C France PV cell. In case of constructing the TDM for the PVW752 cell, the best obtained RMSE value is 1.5182E-04, which is achieved by the proposed approach. The measured and estimated I–V and P–V curves of SDM, DDM, and TDM for R.T.C France and PVW752 PV cells obtained *via* the proposed CapSA are given in Figure 3. The convergence curves of the fitness functions obtained *via* the considered optimizers employed in estimating the SDM parameters of R.T.C France and PVW752 cells are presented in Figure 5. The CapSA achieved the least consumed time to identify the PV parameters during the

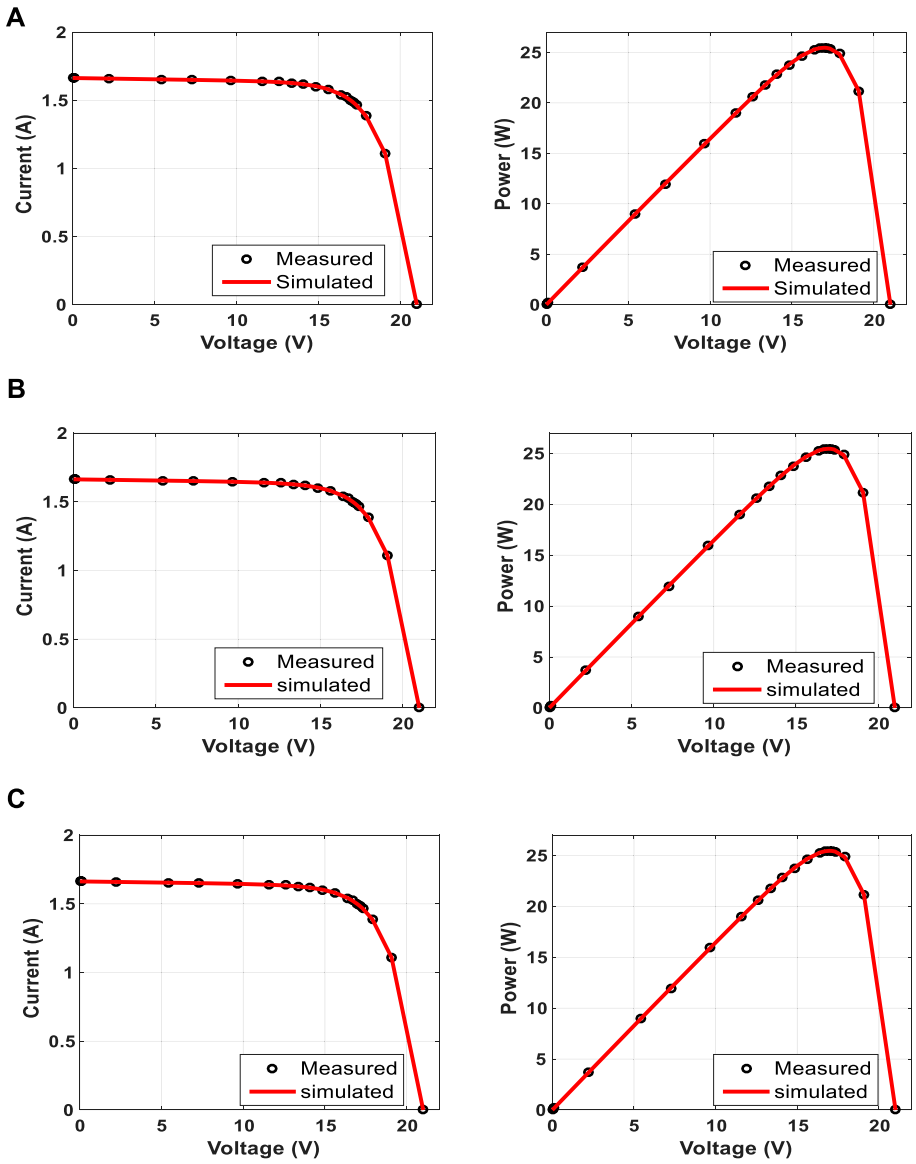

FIGURE 8
Measured and simulated I–V and P–V curves of the STM6-40/36 panel. **(A)** SDM, **(B)** DDM, and **(C)** TDM.

considered number of runs for SDM and DDM of R.T.C of 546.65s and 605.3 s respectively, while SDM and DDM of PVM752 of 591.15 s and 676.3 s, the HAS approach is the longest one in the term of computational time as it required 3092.0 s. The statistical parameters including the minimum, maximum, mean, and standard deviation (Std) are displayed in Table 5 for the PVW752 cell. Regarding the fetched statistical results for the PVM752 PV cell, the proposed CapSA succeeded in achieving the least standard deviations of 8.1938E-18 in constructing the SDM-based circuit. Moreover, it succeeded in achieving the best minimum fitness values for all studied models. The obtained results reveal that the proposed CapSA is the best approach in estimating the optimal parameters of different models for the R.T.C France and PVW752 cells compared to the others considered approaches.

5.2 Case 2: Photovoltaic panel operation at constant weather conditions

In order to confirm the validity of the proposed CapSA, it is applied to identify the SDM, DDM, and TDM unknown

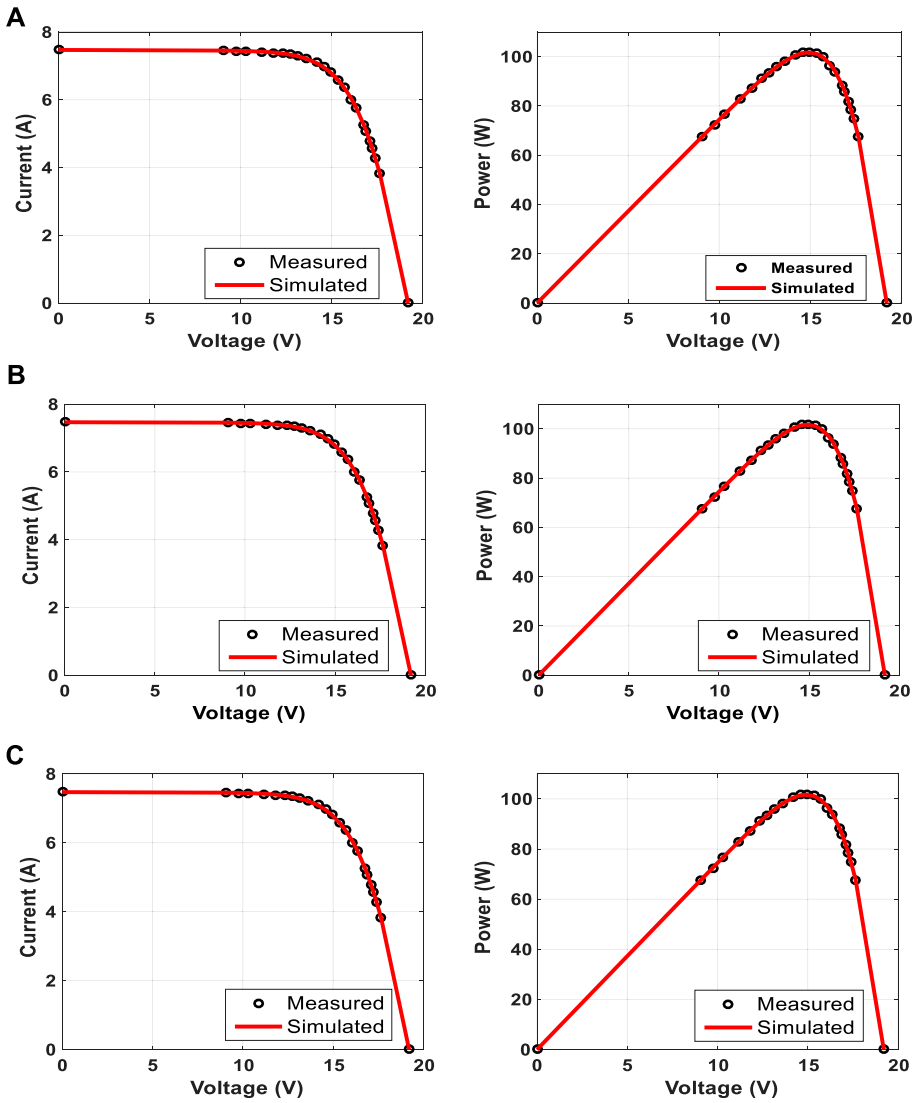

FIGURE 9
Measured and simulated I–V and P–V curves of the STP6-120/36 panel. **(A)** SDM, **(B)** DDM, and **(C)** TDM.

parameters for different PV panels of Photowatt PWP-201, STM6-40/36, and STP6-120/36 PV. The first one is operated at 45°C and 1000W/m^2, the second one is considered at 51°C and 1000W/m^2, and the last one is operated at 55°C and 1000W/m^2. The measured data of I–V for the considered PV panels and electrical characteristics are given in Yu et al. (2019), Long et al. (2020a), Nicaire et al– (2021), and Rezk et al. (2021). The RMSE performance obtained *via* the considered optimizers during the iterative process for SDM is shown in Figure 6. The fitness value and the estimated parameters of SDM obtained *via* the proposed CapSA in comparison with MVO, LAPO, SCA, TSA, EO, and HSA are illustrated in Table 6. The minimum obtained RMSE value is 2.42507E-03 by CapSA and LAPO for the PWP-201 PV panel. The STM6-40/36 and STP6-120/36 best RMSE values of 1.90610E-03 and 1.66006E-02 are obtained *via* CapSA and LAPO, respectively, whereas the worst values are 4.58893E-03 and 3.04560E-02 by SCA. Moreover, Table 7 represents the optimal parameters of DDM; the proposed CapSA achieved the best RMSE values of 2.3306E-03, 1.7309E-03, and 1.6421E-02, whereas the worst RMSE values obtained are 6.5520E-03, 4.5854E-03, and 3.3653E-02 *via* SCA for PWP-201, STM6-40/36, and STP6-120/36, respectively. Furthermore, the optimal parameters of TDM are presented in Table 8, and the best fitness value is 2.3240E-03 achieved by the proposed CapSA for the PWP-201 panel. In addition, it comes first during analyzing STM6-40/

TABLE 9 Statistical parameters of the approaches applied to the STP6-120/36 panel.

Type	Alg	Min	Max	Mean	Std
SDM	CapSA	1.66006031E-02	1.66006031E-02	1.66006031E-02	1.73103476E-16
	MVO	1.66024097E-02	1.71823029E-02	1.67079766E-02	1.31886096E-04
	EO	1.66023515E-02	1.41312204E+00	1.09741140E-01	3.54298215E-01
	LAPO	1.66006031E-02	1.66006070E-02	1.66006033E-02	7.01707815E-10
	HAS	1.67469829E-02	2.89331002E-02	2.18795542E-02	3.29951938E-03
	SCA	3.04559600E-02	1.41312204E+00	3.67790891E-01	4.90546728E-01
	TSA	1.76708961E-02	1.35416081E-01	3.14966322E-02	2.22994547E-02
DDM	CapSA	1.64210210E-02	1.66006031E-02	1.65946171E-02	3.27870560E-05
	MVO	1.66042518E-02	2.30816302E-02	1.74244155E-02	1.33324090E-03
	EO	1.66006223E-02	1.70743634E-02	1.66708141E-02	9.79025158E-05
	LAPO	1.66006031E-02	2.75362809E-02	1.80116544E-02	2.94016381E-03
	HAS	1.66706117E-02	2.83175694E-02	2.17853272E-02	3.46876352E-03
	SCA	3.36525872E-02	1.41312204E+00	5.21312434E-01	5.58982812E-01
	TSA	1.79655604E-02	8.29264560E-02	2.99743805E-02	1.11177170E-02
TDM	CapSA	1.62686170E-02	1.66006031E-02	1.65770491E-02	6.83010194E-05
	MVO	1.66446168E-02	2.66720095E-02	1.99220531E-02	3.20171626E-03
	EO	1.66008254E-02	1.67434923E-02	1.66494190E-02	2.85390862E-05
	LAPO	1.66046480E-02	2.88807595E-02	1.98685592E-02	4.05510059E-03
	HAS	1.68626793E-02	2.62955042E-02	2.23920185E-02	3.12441618E-03
	SCA	3.12403752E-02	1.41312204E+00	4.29131354E-01	4.62263903E-01
	TSA	1.76176013E-02	3.17403058E-01	3.74931732E-02	5.30258003E-02

TABLE 10 Optimal parameters of DDM for the KC200GT PV panel at different temperatures.

Temp	Alg	a_1	a_2	R_s	R_{sh}	I_{dr1}	I_{dr2}	I_g	RMSE
25 °C	CapSA	1.26273	1.05910	0.26322	348.3808	4.117E-08	4.206E-10	8.2162	3.4440E-04
	MVO	1.27003	1.95728	0.23996	265.0288	6.147E-08	1.354E-06	8.2417	2.3564E-02
	EO	1.23485	1.99093	0.25587	499.8649	3.723E-08	0.000E+00	8.2050	4.9701E-03
	LAPO	1.76495	1.21192	0.26052	331.1295	2.534E-08	2.575E-08	8.2189	1.0895E-03
	HAS	1.37281	1.72957	0.19924	499.9444	2.083E-07	1.790E-06	8.2609	6.3185E-02
	SCA	1.00000	1.73907	0.11678	347.1051	0.000E+00	1.000E-05	8.3055	1.0526E-01
	TSA	1.22437	2.00000	0.25770	317.0538	3.158E-08	6.036E-14	8.2313	8.9497E-03
50 °C	CapSA	1.21142	1.00000	0.26161	304.4519	6.282E-07	2.997E-10	8.3011	1.5617E-03
	MVO	1.11396	1.63365	0.26920	312.8954	1.285E-07	6.877E-06	8.3033	3.4934E-03
	EO	1.21338	1.99964	0.26033	338.6095	6.551E-07	2.059E-07	8.2973	2.0672E-03
	LAPO	1.20860	1.56881	0.26138	303.5788	6.137E-07	9.209E-09	8.3012	1.5624E-03
	HAS	1.38901	1.38327	0.21411	499.9674	4.687E-07	4.487E-06	8.3104	3.5727E-02
	SCA	1.42544	1.31795	0.20809	147.0569	0.000E+00	2.403E-06	8.3676	8.2553E-02
	TSA	2.00000	1.23275	0.25051	402.3368	3.290E-06	8.448E-07	8.2898	1.3263E-02
75 °C	CapSA	1.23233	1.23233	0.25567	383.9171	2.601E-06	1.000E-05	8.3735	6.6008E-03
	MVO	1.21299	1.46814	0.26009	338.9426	9.989E-06	1.865E-06	8.3771	7.3468E-03
	EO	1.20996	1.30616	0.25617	390.0654	7.632E-06	6.025E-06	8.3733	6.6124E-03
	LAPO	1.22437	1.28251	0.25574	381.8038	1.000E-05	2.857E-06	8.3737	6.6045E-03
	HAS	1.19374	1.28760	0.25624	388.8589	4.988E-06	8.727E-06	8.3719	6.7135E-03
	SCA	2.00000	1.19475	0.25724	235.9206	0.000E+00	8.317E-06	8.3954	3.2817E-02
	TSA	1.21966	1.21823	0.25814	352.8420	7.178E-06	3.739E-06	8.3751	9.3873E-03

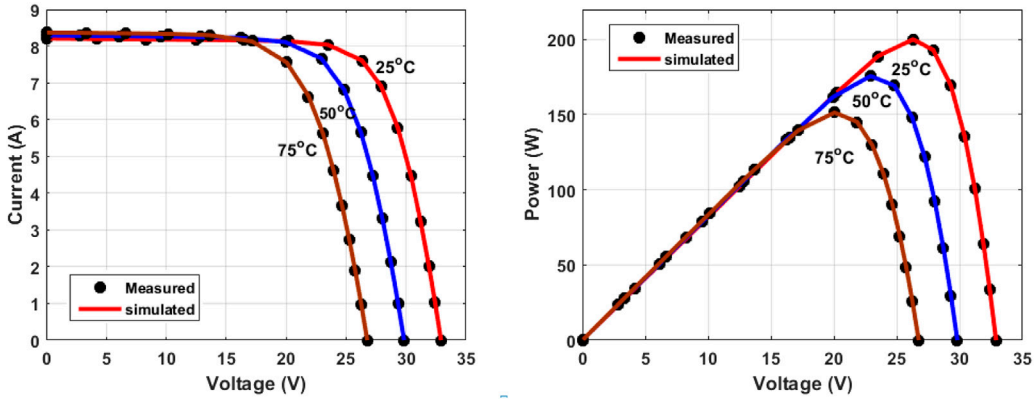

FIGURE 10
I–V and P–V curves of KC200GT at different temperatures.

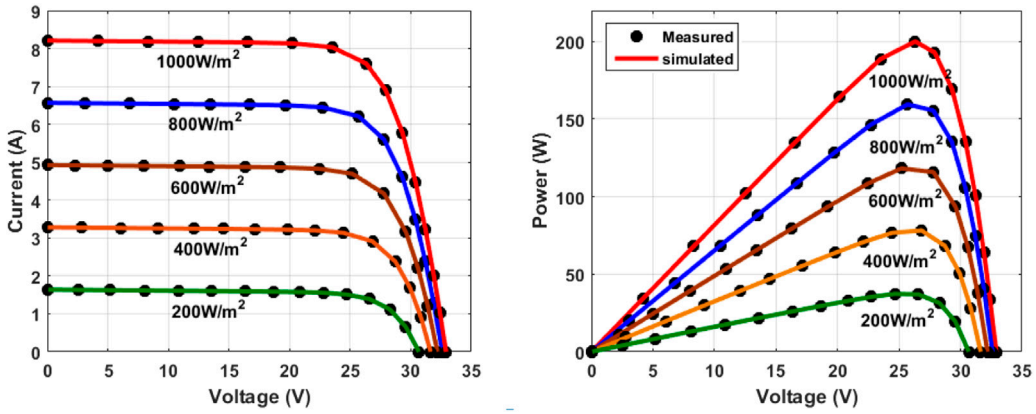

FIGURE 11
Measured and simulated I–V and P–V curves of KC200GT at different irradiances.

36 and STP6-120/36 panels achieving fitness values of 1.7309E-3 and 1.6269E-2, respectively. On the other hand, the SCA came in the last rank with 7.2495E-3, 4.6561E-3, and 3.1240E-2 for PWP-201, STM6-40/36, and STP6-120/36, respectively. To confirm the efficiency and reliability of the proposed CapSA, Figures 7–9 show the measured and simulated I–V and P–V curves obtained *via* the proposed approach; the points coincide with each other in the curves, and this confirms the efficiency of the proposed CapSA. The statistical analyses in such case are tabulated in Table 9, where the CapSA for STP6-120/36 achieved the least mean value of 1.6600603E-02 and standard of 1.73103476E-16 for SDM.

The proposed CapSA achieved great performance by getting estimated curves that are closely matched to the experimental ones; this affirms its competence in such cases.

5.3 Case 3: Photovoltaic panel operation at variable weather conditions

The proposed CapSA is applied to construct the DDM of the KC200GT PV panel operated at different weather conditions. The electrical properties of the panel and the measured data of I–V are presented in Arias García and Pérez Abril (2020). The identified parameters and RMSE values under different temperatures of 25°C, 50°C, and 75°C and irradiance of 1000W/m^2 are tabulated in Table 10. The proposed CapSA achieved the best RMSE values of 3.4440E-04, 1.5617E-03, and 6.6008E-03 during operation at 25°C, 50°C, and 75°C, respectively. The measured and simulated data of I–V and P–V curves obtained by the proposed CapSA at different temperatures and irradiance of 1000W/m^2 are presented in

TABLE 11 Statistical parameters of the optimizers applied on KC200GT at different temperatures.

Temp	Alg	Min	Max	Mean	Std
25 °C	CapSA	3.444036E-04	6.568450E-04	3.758961E-04	6.540437E-05
	MVO	2.356361E-02	1.133120E-01	7.416764E-02	3.016939E-02
	EO	4.970076E-03	2.281323E-02	1.020033E-02	3.974617E-03
	LAPO	1.089528E-03	5.709756E-02	8.494519E-03	1.099060E-02
	HAS	6.318501E-02	9.628150E-02	8.525733E-02	7.387344E-03
	SCA	1.052649E-01	1.936627E+00	4.277749E-01	5.132830E-01
	TSA	8.949739E-03	2.304880E-01	7.388706E-02	4.653636E-02
50 °C	CapSA	1.561721E-03	1.621982E-03	1.564958E-03	1.136903E-05
	MVO	3.493384E-03	6.382028E-02	4.396100E-02	1.493156E-02
	EO	2.067201E-03	3.600570E-01	1.697596E-02	6.480282E-02
	LAPO	1.562391E-03	1.249924E-02	3.042621E-03	2.642205E-03
	HAS	3.572709E-02	5.301741E-02	4.435417E-02	4.141684E-03
	SCA	8.255257E-02	1.836699E+00	3.866787E-01	2.898690E-01
	TSA	1.326310E-02	3.234687E-01	5.280451E-02	7.356309E-02
75 °C	CapSA	6.600763E-03	6.641768E-03	6.602140E-03	7.484815E-06
	MVO	7.346834E-03	5.503000E-02	2.683364E-02	1.564604E-02
	EO	6.612390E-03	8.329508E-03	6.982191E-03	4.972071E-04
	LAPO	6.604509E-03	7.556521E-03	6.704904E-03	2.377387E-04
	HAS	6.713519E-03	1.335816E-02	8.526225E-03	1.653807E-03
	SCA	3.281675E-02	5.000065E-01	3.510030E-01	1.857197E-01
	TSA	9.387263E-03	5.421342E-02	2.197971E-02	1.016525E-02

TABLE 12 Statistical parameters of the optimizers applied on KC200GT at different irradiances.

Type	Alg	Min	Max	Mean	Std
800W/m^2	CapSA	3.135527E-04	4.986875E-04	3.387959E-04	3.229922E-05
	MVO	2.764607E-02	8.004170E-02	6.443408E-02	1.689657E-02
	EO	1.153687E-02	2.926776E-03	1.107292E-01	1.903401E-02
	LAPO	2.909586E-03	8.743885E-04	9.815111E-03	2.506060E-03
	HAS	6.468453E-02	5.417470E-02	7.271330E-02	5.045976E-03
	SCA	1.353808E-01	7.391964E-02	1.500957E-01	1.722395E-02
	TSA	5.588023E-02	1.474472E-02	1.125553E-01	1.980739E-02
600W/m^2	CapSA	2.655815E-04	6.139179E-04	3.090731E-04	6.000390E-05
	MVO	1.208970E-02	5.762172E-02	4.322857E-02	1.284707E-02
	EO	3.486157E-03	5.576775E-02	1.451801E-02	1.883175E-02
	LAPO	6.475980E-04	9.930363E-03	2.890841E-03	2.190327E-03
	HAS	3.775617E-02	5.151757E-02	4.539985E-02	2.908935E-03
	SCA	5.657250E-02	7.322014E-02	6.235295E-02	4.475244E-03
	TSA	1.739688E-02	5.622447E-02	3.553514E-02	9.071938E-03

(Continued on following page)

TABLE 12 (*Continued*) Statistical parameters of the optimizers applied on KC200GT at different irradiances.

Type	Alg	Min	Max	Mean	Std
400W/m^2	CapSA	1.787039E-04	2.240823E-04	1.850509E-04	1.131600E-05
	MVO	6.837013E-03	5.114658E-02	2.698709E-02	1.186716E-02
	EO	2.632530E-03	2.477385E-02	1.243201E-02	1.027185E-02
	LAPO	3.015540E-04	2.419746E-02	2.610697E-03	4.550485E-03
	HAS	1.238208E-02	2.587089E-02	2.269038E-02	2.717497E-03
	SCA	2.532240E-02	7.150308E-01	5.454065E-02	1.248065E-01
	TSA	8.522987E-03	2.511727E-02	1.975371E-02	4.106596E-03
200W/m^2	CapSA	2.306877E-04	2.384415E-04	2.329307E-04	1.273499E-06
	MVO	2.539602E-03	5.529677E-02	3.688713E-02	2.030515E-02
	EO	3.759840E-04	5.483972E-03	2.434542E-03	2.352910E-03
	LAPO	2.390938E-04	5.816649E-03	1.301924E-03	1.785978E-03
	HAS	4.939335E-03	9.515761E-03	6.781784E-03	1.232729E-03
	SCA	6.509237E-03	3.397564E-01	3.398551E-02	8.320434E-02
	TSA	1.580553E-03	7.815697E-03	5.448930E-03	1.107577E-03

The obtained results proved that the proposed CapSA is efficient in extracting the optimal parameters of different models for the PV cell/panel, as it outperformed the other considered approaches in all studied cases.

Figure 10. Figure 11 illustrates the I–V and P–V curves of the measured and simulated data obtained by the proposed CapSA at 25°C and different irradiances of 1000W/m^2, 800W/m^2, 600W/m^2, 400W/m^2, and 200W/m^2. The simulated data are closely matched to the measured points. Additionally, the statistical analysis under different temperatures and irradiances are tabulated in Table 11 and Table 12, respectively.

6 Conclusion

This study proposed an efficient approach incorporating the capuchin search algorithm (CapSA) to identify the unknown parameters of SDM-, DDM-, and TDM-based circuits of different PV cells and panels. The considered fitness function is the root mean square error between the measured and simulated currents. R.T.C France, PVM752, PWP-201, STM6-40/36, STP6-120/36, and KC200GT are the cells and panels considered in the analysis. Comparison to a multiverse optimizer (MVO), lighting attachment procedure optimization (LAPO), sine–cosine algorithm (SCA), tunicate swarm algorithm (TSA), equilibrium optimizer (EO), and harmony search algorithm (HSA) is conducted. The proposed approach achieved several features as follow:

1) Regarding the SDM circuit, the proposed CapSA outperformed all considered optimizers achieving the best RMSE values of 9.86022E-04, 2.27804E-04, 2.42507E-03, 1.90610E-03, and 1.66006E-02 with the fastest computational times of 546.6 s, 591.1 s, 517.5 s, 542.8 s, and 445.4 s for the R.T.C France cell, PVW752 cell, PWP-201 panel, STM6-40/36 panel, and STP6-120/36 panel, respectively.
2) For DDM, the proposed CapSA achieved the best fitness values of 9.8248E-04, 1.3808E-04, 2.3306E-03, 1.7309E-03, and 1.6421E-02 with the best computational times of 605.3 s, 676.5 s, 535.0 s, 548.7 s, and 536.4 s for the R.T.C France cell, PVW752 cell, PWP-201 panel, STM6-40/36 panel, and STP6-120/36 panel, respectively.
3) In the case of TDM, the proposed approach achieved RMSE values of 9.8248E-04, 1.5182E-04, 2.3240E-03, 1.7309E-3, and 1.6269E-2 for the R.T.C France cell, PVW752 cell, PWP-201 panel, STM6-40/36 panel, and STP6-120/36 panel, respectively.
4) For the KC200GT panel, the CapSA outperformed the others and achieved the best RMSE values of 3.4440E-04, 1.5617E-03, and 6.6008E-03 at 25°C, 50°C, and 75°C, respectively.

The obtained results confirmed the competence and preference of the proposed CapSA in establishing a reliable equivalent circuit for the PV cell/panel operated at different weather conditions. Establishing a dynamic model of the PV panel is recommended in the future; moreover, enhancing the CapSA approach *via* hybridization with novel approaches will be considered in future studies.

Data availability statement

The original contributions presented in the study are included in the article/Supplementary materials,

further inquiries can be directed to the corresponding author.

Author contributions

Conceptualization, HA and AF; methodology, ME and MA-D; software, ME and AA; validation, AF, ME, and AA; formal analysis, HA; investigation, HA and ME; resources, MA-D; data curation, AF and MA-D; writing—original draft preparation, HA and ME; writing—review and editing, AF and MA-D; visualization, AF; supervision, AA. All authors have read and agreed to the published version of the manuscript.

Funding

The authors acknowledge the support of King Fahd University of Petroleum and Minerals, Saudi Arabia.

Conflict of interest

The authors declare that the research was conducted in the absence of any commercial or financial relationships that could be construed as a potential conflict of interest.

Publisher's note

All claims expressed in this article are solely those of the authors and do not necessarily represent those of their affiliated organizations, or those of the publisher, the editors, and the reviewers. Any product that may be evaluated in this article, or claim that may be made by its manufacturer, is not guaranteed or endorsed by the publisher.

Supplementary material

The Supplementary Material for this article can be found online at: https://www.frontiersin.org/articles/10.3389/fenrg.2022.1028816/full#supplementary-material

References

Abdel-Basset, M., Mohamed, R., Chakrabortty, R. K., Ryan, M. J., and El-Fergany, A. (2021). An improved artificial jellyfish search optimizer for parameter identification of photovoltaic models. *Energies* 14, 1867. doi:10.3390/en14071867

Abdelminaam, D. S., Said, M., and Houssein, E. H. (2021). Turbulent flow of water-based optimization using new objective function for parameter extraction of six photovoltaic models. *IEEE Access* 9, 35382–35398. doi:10.1109/ACCESS.2021.3061529

Ahmadianfar, I., Gong, W., Heidari, A. A., Golilarz, N. A., Samadi-Koucheksaraee, A., and Chen, H. (2021). Gradient-based optimization with ranking mechanisms for parameter identification of photovoltaic systems. *Energy Rep.* 7, 3979–3997. doi:10.1016/j.egyr.2021.06.064

Alam, D. F., Yousri, D. A., and Eteiba, M. B. (2015). Flower Pollination Algorithm based solar PV parameter estimation. *Energy Convers. Manag.* 101, 410–422. doi:10.1016/j.enconman.2015.05.074

Arias García, R. M., and Pérez Abril, I. (2020). Photovoltaic module model determination by using the Tellegen's theorem. *Renew. Energy* 152, 409–420. doi:10.1016/j.renene.2020.01.048

Askarzadeh, A., and Rezazadeh, A. (2013). Artificial bee swarm optimization algorithm for parameters identification of solar cell models. *Appl. Energy* 102, 943–949. doi:10.1016/j.apenergy.2012.09.052

Ayang, A., Wamkeue, R., Ouhrouche, M., Djongyang, N., Essiane Salomé, N., Pombe, J. K., et al. (2019). Maximum likelihood parameters estimation of single-diode model of photovoltaic generator. *Renew. Energy* 130, 111–121. doi:10.1016/j.renene.2018.06.039

Bertalero, G., Addebito, P., Bancario, C. C., and Cliente, C. A. L. (2021). Parameters extraction of three diode photovoltaic models using boosted LSHADE algorithm and Newton Raphson method. 224 120–136. doi:10.1016/j.energy.2021.120136

Braik, M., Sheta, A., and Al-Hiary, H. (2021). A novel meta-heuristic search algorithm for solving optimization problems: Capuchin search algorithm. *Neural comput. Appl.* 33, 2515–2547. doi:10.1007/s00521-020-05145-6

Ćalasan, M., Abdel Aleem, S. H. E., and Zobaa, A. F. (2020). On the root mean square error (RMSE) calculation for parameter estimation of photovoltaic models: A novel exact analytical solution based on Lambert W function. *Energy Convers. Manag.* 210, 112716. doi:10.1016/j.enconman.2020.112716

Chen, X., Xu, B., Mei, C., Ding, Y., and Li, K. (2018). Teaching–learning–based artificial bee colony for solar photovoltaic parameter estimation. *Appl. Energy* 212, 1578–1588. doi:10.1016/j.apenergy.2017.12.115

El-Fergany, A. A. (2021). Parameters identification of PV model using improved slime mould optimizer and Lambert W-function. *Energy Rep.* 7, 875–887. doi:10.1016/j.egyr.2021.01.093

Fathy, A., and Rezk, H. (2017). Parameter estimation of photovoltaic system using imperialist competitive algorithm. *Renew. Energy* 111, 307–320. doi:10.1016/j.renene.2017.04.014

Gao, X., Cui, Y., Hu, J., Xu, G., Wang, Z., Qu, J., et al. (2018). Parameter extraction of solar cell models using improved shuffled complex evolution algorithm. *Energy Convers. Manag.* 157, 460–479. doi:10.1016/j.enconman.2017.12.033

Ginidi, A., Ghoneim, S. M., Elsayed, A., El-Sehiemy, R., Shaheen, A., and El-Fergany, A. (2021). Gorilla troops optimizer for electrically based single and double-diode models of solar photovoltaic systems. *Sustainability* 13, 9459. doi:10.3390/su13169459

Gnetchejo, P. J., Ndjakomo Essiane, S., Dadjé, A., and Ele, P. (2021). A combination of Newton-Raphson method and heuristics algorithms for parameter estimation in photovoltaic modules. *Heliyon* 7, e06673. doi:10.1016/j.heliyon.2021.e06673

Ibrahim, I. A., Hossain, M. J., Duck, B. C., and Nadarajah, M. (2020). An improved wind driven optimization algorithm for parameters identification of a triple-diode photovoltaic cell model. *Energy Convers. Manag.* 213, 112872. doi:10.1016/j.enconman.2020.112872

Ismaeel, A. A. K., Houssein, E. H., Oliva, D., and Said, M. (2021). Gradient-based optimizer for parameter extraction in photovoltaic models. *IEEE Access* 9, 13403–13416. doi:10.1109/ACCESS.2021.3052153

Jiang, Y., Luo, Q., and Zhou, Y. (2022). Improved gradient-based optimizer for parameters extraction of photovoltaic models. *IET Renew. Power Gen.* 16, 1602–1622. doi:10.1049/rpg2.12465

Jiao, S., Chong, G., Huang, C., Hu, H., Wang, M., Heidari, A. A., et al. (2020). Orthogonally adapted Harris hawks optimization for parameter estimation of photovoltaic models. *Energy* 203, 117804. doi:10.1016/j.energy.2020.117804

Lekouaghet, B., Boukabou, A., and Boubakir, C. (2021). Estimation of the photovoltaic cells/modules parameters using an improved Rao-based chaotic optimization technique. *Energy Convers. Manag.* 229, 113722. doi:10.1016/j.enconman.2020.113722

Long, W., Cai, S., Jiao, J., Xu, M., and Wu, T. (2020a). A new hybrid algorithm based on grey wolf optimizer and cuckoo search for parameter extraction of solar photovoltaic models. *Energy Convers. Manag.* 203, 112243. doi:10.1016/j.enconman.2019.112243

Long, W., Wu, T., Jiao, J., Tang, M., and Xu, M. (2020b). Refraction-learning-based whale optimization algorithm for high-dimensional problems and parameter estimation of PV model. *Eng. Appl. Artif. Intell.* 89, 103457. doi:10.1016/j.engappai.2019.103457

Long, W., Wu, T., Xu, M., Tang, M., and Cai, S. (2021). Parameters identification of photovoltaic models by using an enhanced adaptive butterfly optimization algorithm. *Energy* 229, 120750. doi:10.1016/j.energy.2021.120750

Low, K. S., and Soon, J. J. (2012). Photovoltaic model identification using particle swarm optimization with inverse barrier constraint. *IEEE Trans. Power Electron.* 27, 3975–3983. doi:10.1109/tpel.2012.2188818

Mokeddem, D. (2021). Parameter extraction of solar photovoltaic models using enhanced levy flight based grasshopper optimization algorithm. *J. Electr. Eng. Technol.* 16, 171–179. doi:10.1007/s42835-020-00589-1

Mostafa, M., Rezk, H., Aly, M., and Ahmed, E. M. (2020). A new strategy based on slime mould algorithm to extract the optimal model parameters of solar PV panel. *Sustain. Energy Technol. Assessments* 42, 100849. doi:10.1016/j.seta.2020.100849

Nicaire, N. F., Steve, P. N., Salome, N. E., and Grégroire, A. O. (2021). Parameter estimation of the photovoltaic system using bald eagle search (BES) algorithm. *Int. J. Photoenergy* 2021, 1–20. doi:10.1155/2021/4343203

Pourmousa, N., Ebrahimi, S. M., Malekzadeh, M., and Alizadeh, M. (2019). Parameter estimation of photovoltaic cells using improved Lozi map based chaotic optimization Algorithm. *Sol. Energy* 180, 180–191. doi:10.1016/j.solener.2019.01.026

Premkumar, M., Jangir, P., Elavarasan, R. M., and Sowmya, R. (2021a). Opposition decided gradient-based optimizer with balance analysis and diversity maintenance for parameter identification of solar photovoltaic models. *J. Ambient. Intell. Humaniz. Comput.* doi:10.1007/s12652-021-03564-4

Premkumar, M., Jangir, P., Jebaseelan, S. D. T. S., Elavarasan, R. M., Chen, H., Kumar, C., et al. (2022). Constraint estimation in three-diode solar photovoltaic model using Gaussian and Cauchy mutation-based hunger games search optimizer and enhanced Newton–Raphson method. *IET Renew. Power Gen.* 16, 1733–1772. doi:10.1049/rpg2.12475

Premkumar, M., Jangir, P., Ramakrishnan, C., Nalinipriya, G., Alhelou, H. H., and Kumar, B. S. (2021b). Identification of solar photovoltaic model parameters using an improved gradient-based optimization algorithm with chaotic drifts. *IEEE Access* 9, 62347–62379. doi:10.1109/ACCESS.2021.3073821

Premkumar, M., Jangir, P., Sowmya, R., Elavarasan, R. M., and Kumar, B. S. (2021c). Enhanced chaotic JAYA algorithm for parameter estimation of photovoltaic cell/modules. *ISA Trans.* 116, 139–166. doi:10.1016/j.isatra.2021.01.045

Ram, J. P., Babu, T. S., Dragicevic, T., and Rajasekar, N. (2017). A new hybrid bee pollinator flower pollination algorithm for solar PV parameter estimation. *Energy Convers. Manag.* 135, 463–476. doi:10.1016/j.enconman.2016.12.082

Ramadan, A., Kamel, S., Hassan, M. H., Khurshaid, T., and Rahmann, C. (2021a). An improved bald eagle search algorithm for parameter estimation of different photovoltaic models. *Processes* 9, 1127. doi:10.3390/pr9071127

Ramadan, A., Kamel, S., Hussein, M. M., and Hassan, M. H. (2021b). A new application of chaos game optimization algorithm for parameters extraction of three diode photovoltaic model. *IEEE Access* 9, 51582–51594. doi:10.1109/ACCESS.2021.3069939

Reddy, S. S., and Yammani, C. (2021). A novel two step method to extract the parameters of the single diode model of Photovoltaic module using experimental Power–Voltage data. *Opt. (Stuttg).* 248, 167977. doi:10.1016/j.ijleo.2021.167977

Rezaee Jordehi, A. (2018). Enhanced leader particle swarm optimisation (ELPSO): An efficient algorithm for parameter estimation of photovoltaic (PV) cells and modules. *Sol. Energy* 159, 78–87. doi:10.1016/j.solener.2017.10.063

Rezk, H., Babu, T. S., Al-Dhaifallah, M., and Ziedan, H. A. (2021). A robust parameter estimation approach based on stochastic fractal search optimization algorithm applied to solar PV parameters. *Energy Rep.* 7, 620–640. doi:10.1016/j.egyr.2021.01.024

Said, M., Shaheen, A. M., Ginidi, A. R., El-Sehiemy, R. A., Mahmoud, K., Lehtonen, M., et al. (2021). Estimating parameters of photovoltaic models using accurate turbulent flow of water optimizer. *Processes* 9, 627. doi:10.3390/pr9040627

Sattar, M. A. El, Al Sumaiti, A., Ali, H., and Diab, A. A. Z. (2021). Marine predators algorithm for parameters estimation of photovoltaic modules considering various weather conditions. *Neural comput. Appl.* 33, 11799–11819. doi:10.1007/s00521-021-05822-0

Şentürk, A. (2018). New method for computing single diode model parameters of photovoltaic modules. *Renew. Energy* 128, 30–36. doi:10.1016/j.renene.2018.05.065

Shaheen, A. M., Ginidi, A. R., El-Sehiemy, R. A., and Ghoneim, S. S. M. (2021). A forensic-based investigation algorithm for parameter extraction of solar cell models. *IEEE Access* 9, 1–20. doi:10.1109/ACCESS.2020.3046536

Sharma, A., Sharma, A., Moshe, A., Raj, N., and Pachauri, R. K. (2021). An effective method for parameter estimation of solar PV cell using grey-wolf optimization technique. *Int. J. Math. Eng. Manag. Sci.* 6, 911–931. doi:10.33889/ijmems.2021.6.3.054

Stornelli, V., Muttillo, M., de Rubeis, T., and Nardi, I. (2019). A new simplified five-parameter estimation method for single-diode model of photovoltaic panels. *Energies* 12, 4271. doi:10.3390/en12224271

Wang, J., Yang, B., Li, D., Zeng, C., Chen, Y., Guo, Z., et al. (2021). Photovoltaic cell parameter estimation based on improved equilibrium optimizer algorithm. *Energy Convers. Manag.* 236, 114051. doi:10.1016/j.enconman.2021.114051

Wang, L., and Huang, C. (2018). A novel Elite Opposition-based Jaya algorithm for parameter estimation of photovoltaic cell models. *Opt. (Stuttg).* 155, 351–356. doi:10.1016/j.ijleo.2017.10.081

Yang, B., Wang, J., Zhang, X., Yu, T., Yao, W., Shu, H., et al. (2020). Comprehensive overview of meta-heuristic algorithm applications on PV cell parameter identification. *Energy Convers. Manag.* 208, 112595. doi:10.1016/j.enconman.2020.112595

Yousri, D., Rezk, H., and Fathy, A. (2020). Identifying the parameters of different configurations of photovoltaic models based on recent artificial ecosystem-based optimization approach. *Int. J. Energy Res.* 44, 11302–11322. doi:10.1002/er.5747

Yu, K., Liang, J. J., Qu, B. Y., Cheng, Z., and Wang, H. (2018). Multiple learning backtracking search algorithm for estimating parameters of photovoltaic models. *Appl. Energy* 226, 408–422. doi:10.1016/j.apenergy.2018.06.010

Yu, K., Qu, B., Yue, C., Ge, S., Chen, X., and Liang, J. (2019). A performance-guided JAYA algorithm for parameters identification of photovoltaic cell and module. *Appl. Energy* 237, 241–257. doi:10.1016/j.apenergy.2019.01.008

Yu, S., Chen, Z., Heidari, A. A., Zhou, W., Chen, H., and Xiao, L. (2022). Parameter identification of photovoltaic models using a sine cosine differential gradient based optimizer. *IET Renew. Power Gen.* 16, 1535–1561. doi:10.1049/rpg2.12451

Zeng, F., Shu, H., Wang, J., Chen, Y., and Yang, B. (2021). Parameter identification of PV cell via adaptive compass search algorithm. *Energy Rep.* 7, 275–282. doi:10.1016/j.egyr.2021.01.069

Zhang, Y., Jin, Z., and Mirjalili, S. (2020). Generalized normal distribution optimization and its applications in parameter extraction of photovoltaic models. *Energy Convers. Manag.* 224, 113301. doi:10.1016/j.enconman.2020.113301